Tanshinone IIA as a therapy for PCOS via FOS/JUN/TP53 axis: Evidence from network pharmacology of Bajitian-Danshen pair

Honglin Liu [a,1], Jianhua Zhou [a,1], Jiani Xie [a,1], Limin Fan [b,1], Yue Xia [a], Xia Peng [a], Huilan Du [c,*], Xiaorong Ni [a,*]

[a] *Department of Gynecology, Shanghai Municipal Hospital of Traditional Chinese Medicine, Shanghai University of Traditional Chinese Medicine, Shanghai 200071, China*
[b] *The Institute for Biomedical Engineering and Nano Science, Tongji University School of Medicine, NO1239, Siping Road, Shanghai, 200092, China*
[c] *Hebei University of Chinese Medicine, No. 3, Xingyuan Road, Luquan Economic Development Zone, Hebei Province, Shijiazhuang City 050200, China*

ARTICLE INFO

ABSTRACT

Polycystic ovary syndrome (PCOS) is a common disease affecting women of reproductive age; there is a need for interventions to address this condition. Herein, the network pharmacology approach was used to explore the potential of combining *Morindae Officinalis Radix* (Bajitian) and *Radix Salviae* (Danshen) for treating PCOS. The bioactive ingredients of the Bajitian-Danshen pair were identified and used for predicting potential therapeutic target genes. Genes related to PCOS were predicted by keyword search from various databases and intersected with the predicted targets of the active components of the Bajitian-Danshen pair to obtain key target genes, which were used for building the "active compound-target gene" pharmacological network. The TCGAbiolinks package in the R environment was used for functional enrichment analysis. In addition, *in vivo* and *in vitro* PCOS models were established to explore the effect of the key bioactive compound on the treatment of PCOS and the underlying mechanisms. Histopathological analysis was performed by hematoxylin and eosin staining, while the detection of hormone and cytokine levels was performed by conducting ELISA. Immunofluorescence and western blotting were used for protein expression analysis. Tanshinone IIA (Tan-IIA) was found to be the ingredient with the highest number of target genes. The protein–protein interaction (PPI) network analysis revealed that JUN, FOS, TP53, PTGS2, MMP9, CDKN1A, BCL2, DPP4, and CASP3 were key target genes of Tan-IIA in PCOS. The docking analysis showed the interaction of Tan-IIA with FOS. Thus, the therapeutic potential of Tan-IIA in PCOS and its effect on FOS were evaluated experimentally. A rat model of PCOS was established and subsequently treated with Tan-IIA. Tan-IIA treatment attenuated the deleterious effects associated with PCOS and down-regulated TP53, FOS and JUN mRNA and protein expression levels in the ovarian tissue of PCOS rats. In addition, the activation of FOS expression was followed by the exacerbation of the deleterious effect of PCOS and increased expression levels of JUN and TP53. Thus, we concluded that the Bajitian-Danshen pair, especially the Tan-IIA ingredient, counteracts PCOS-induced damage by possibly regulating the FOS/JUN/TP53 axis.

1. Introduction

Polycystic ovary syndrome (PCOS) is a complex condition encountered in about 10–15 % of women of reproductive age and is associated with clinical anovulatory infertility (Hart, 2008, Azziz et al., 2016). The treatment strategies for PCOS remain unclear due to the unelucidated pathogenic mechanisms of this disease (Bednarska and Siejka, 2017, Jin and Xie, 2018). Moreover, most of the therapeutic options are based on

drugs such as metformin and hormones with unsatisfactory results and severe side effects, including nausea, headaches, diarrhea, muscle pain, myolysis, and abdominal cramping (Bednarska and Siejka, 2017, Jin and Xie, 2018). Thus, studies are encouraged to understand the pathogenesis underlying PCOS and find alternative treatment approaches.

Radix Salviae (Danshen) is a well-characterized traditional Chinese medicine (TCM) that has attracted much attention in the scientific community due to its therapeutic properties. Danshen contains

tremendous bioactive ingredients and has been reported to be effective in a panoply of diseases, including diabetes (Orgah et al., 2020, Liu et al., 2022a) cardiovascular (Wang et al., 2017, Li et al., 2018, Orgah et al., 2020, Kumar et al., 2021) and neurodegenerative (Hügel and Jackson, 2014, Guo et al., 2020, Wang et al., 2020a, Tan et al., 2021, Zhang et al., 2021a) diseases, and numerous cancers such as colorectal cancer, breast cancer, gastric cancer, and liver cancer (Yang et al., 2010, Lin et al., 2017, Wu et al., 2017a, Wu et al., 2017b, Yang et al., 2017, Lin et al., 2019, Wang et al., 2019). Some previous reports indicated that Danshen might be effective in treating and preventing PCOS (Amini et al., 2020, Yu et al., 2023). Few of the active ingredients of Danshen, including cryptotanshinone (24–28) and Tan-IIA (29), have been confirmed to be efficient against PCOS. However, the most active ingredients of Danshen in PCOS have not been explored. Further in-depth analyses are needed to certify the most effective ingredients of Danshen for PCOS treatment.

Morindae Officinalis Radix (Bajitian) is a traditional herbal medicine used for strengthening bone and muscularity, tonifying the kidney, and dissipating wind – dampness (Kang et al., 2021). Bajitian is also a widespread dietary supplement used in healthcare (Kang et al., 2021, Jiang et al., 2022). Ingredients from Bajitian exert numerous bioactive activities such as anti-inflammation, anti-depressant, anti-osteoporosis, immune-regulatory, pro-fertility, and antioxidant activities (Wu et al., 2023). However, the effect of Bajitian on PCOS has not been verified so far, so an in-depth study is needed. Combination pharmacology is an important discipline allowing the improvement of the therapeutic effect of combined drugs in the treatment of various diseases (Wang et al., 2021).

Dr. Xiaorong Ni (the corresponding author of the present study) has found great success in treating PCOS by customizing a basic formula including Bajitian and Danshen. Bajitian is known to strengthen tendons and bones, reinforce kidney yang, and dispel wind and dampness (Wu et al., 2015, Zhang et al., 2020, Ma et al., 2021, Liu et al., 2022b, Wu et al., 2022a, Zhang et al., 2022a, Zhang et al., 2022b). Meanwhile, Danshen promotes blood circulation, relieves pain, clears the heart, and cools the blood to resolve abscesses (Xin et al., 2021). Research has shown that these herbs and their chemical components can reduce inflammatory cascades, exhibit blood circulation properties, improve glucose metabolism, and reduce insulin resistance (Xie et al., 2015, Shi et al., 2020, Ye et al., 2020, Guo et al., 2021, Ye et al., 2021, Huang et al., 2023). The combination of TCM herbal medicines has been reported to be more effective than single-drug treatment (Shi et al., 2022, Zhang et al., 2022c). Combining Bajitian-Danshen could provide multiple benefits when treating PCOS. The combination of these two herbs can effectively address the root cause and the accompanying symptoms of PCOS. By nourishing the kidney deficiency and eliminating the blood stasis component, this herbal remedy can possibly provide comprehensive relief. Thus, the combination could create synergistic effects, making the treatment more potent and effective. It could also allow for a multi-target approach and enable personalized treatment based on the specific pathological pattern in each patient while minimizing potential side effects and enhancing the overall efficacy of the treatment. However, the combinatory effects of the Bajitian-Danshen pair on the deleterious impact of PCOS have not been extensively explored so far.

Network pharmacology is a discipline integrating bioinformatics, system biology, and high throughput histology and is based on network building via a series of appropriate databases, uncovering key ingredients and their targets in specific diseases, and experimental validation to ascertain the credibility of the constructed network (Dong et al., 2021, Li et al., 2022a, Nogales et al., 2022, Zhou et al., 2022a). The integration of network pharmacology analysis and TCM has been applied to prioritize disease-gene association and drug-gene-disease interactions (Li and Zhang, 2013, Luo et al., 2020, Gao et al., 2021, Jiashuo et al., 2022). Moreover, molecular docking is a hypothetical approach facilitating the study of interactions and recognition between small molecules and protein receptors by predicting the mode of binding and the degree of affinity (Pinzi and Rastelli, 2019). Network

pharmacology and molecular docking are two complementary methods applicable to TCM research in an integrated way to find new ideas for screening new drugs and studying their mechanisms of action, which could trigger an accelerated transformation in the modernization and internationalization of TCM (Liu et al., 2021b, Zhang et al., 2021b, Wu et al., 2022b).

In our present study, an approach integrating network pharmacology, molecular docking, and experimental validation *in vitro* and *in vivo* was applied to unearth the active ingredients, potential targets, and molecular mechanisms of the Danshen-Bajitian pair against PCOS.

2. Materials and methods

2.1. Reagents

Salvia miltiorrhiza (Danshen) granules and *Eclipta prostrata* (Bajitian) granules were obtained from Jiangyin Tianjiang Pharmaceutical Co., Ltd. Tan-IIA (MR 294.34, >99 % purity) was obtained from Shanghai YuanYe Biotechnology Corporation (Shanghai, China). Human insulin solution (cat. no. I9278) as well as glucose and sucrose assay kit (cat. no. MAK013) were from Sigma-Aldrich (St Louis, MO, USA)). Human chorionic gonadotropin (HCG; cat. no. NBP25954510) was from Novus Biologicals. ELISA kits for follicle-stimulating hormone (FSH) (cat. no. ab108641), LH (cat. no. ab108651), tumor necrosis factor (TNF)-α (cat. no. ab181421), testosterone (cat. no. ab178663) and the glucose oxidase assay kit (cat. no. ab138884) were obtained from Abcam. Pregnant mare serum gonadotrophin (PMSG) was obtained from Ningbo Sansheng Pharmaceutical Co., Ltd. (Ningbo, Zhejiang Province, China), while Bovine serum albumin (BSA; cat. no. SW3015) was from Solarbio Co., Ltd. (Beijing, China). The Dako Real™ Envision™ Detection System was commercially obtained from Dako (cat. no. K500711; Dako; Agilent Technologies, Inc., Santa Clara, CA, USA). Lipofectamine® RNAiMAX transfection reagent (cat. no. 13778150) was commercially acquired from Invitrogen (Shanghai, China). Phorbol 12-myristate 13-acetate (PMA) was commercially provided by Sigma (St. Louis, MO, USA).

2.2. Construction of a database of main active ingredients

The active ingredients of the Bajitian-Danshen pair were identified through the traditional Chinese medicine system pharmacology database and analysis platform (TCMSP, https://lsp.nwu.edu.cn/tcmsp.php). The main active ingredients of the Bajitian-Danshen pair were then selected according to the optimal toxicologic ADME rules reported in the literature (oral bioavailability (OB) ≥ 30 %; drug-like property (DL) ≥ 0.18).

2.3. Potential targets of drug and disease and target classification

All targets of Bajitian-Danshen active ingredients were extracted from the TCMSP database. All the names of targets were converted into gene symbols by using the Uniprot database (https://www.uniprot.org). The keyword "Polycystic Ovary Syndrome" was input into the OMIM database (https://omim.org/), GeneCards database (http://www.genecards.org/), PharmGkb database (https://www.pharmgkb.org/), DrugBank database (https://www.drugbank.ca/) and DisGeNET database (https://www.disgenet.org/) to find genes involved in PCOS pathogenesis. After that, the search results of the five databases were gathered, aggregated, and de-duplicated to obtain the PCOS-related gene list. The Venn diagrams were generated by using the online tool from the domain https://bioinformatics.psb.ugent.be/webtools/Venn/ to get the potential targets of Bajitian-Danshen pair in PCOS.

2.4. Compound-gene network and protein–protein interaction (PPI) network construction

The TCM compound regulatory network was constructed by using

Cytoscape 3.8.0 (https://cytoscape.org/) to obtain the target relationship between the active ingredients and target genes. The protein–protein interaction (PPI) network was generated in STRING (https://string-db.org/). We selected "multiple proteins" in the database, inputted the list of potential targets of Bajitian and Danshen in PCOS with the species limited to "*Homo sapiens*" and confidence scores ≥ 0.4, and exported the PPI data. We analyzed the topology of the PPI network by using the CytoNCA plug-in in Cytoscape 3.8.0. We selected gene to carry out topology analysis on three parameters of degree centrality (DC), betweenness centrality (BC), and closeness centrality (CC) with the filter criteria limited to the top of 50 % according to the centrality of nodes to evaluate the importance of target genes.

2.5. Functional analysis of target genes

Functional enrichment analysis of targets and the visualization of enrichment terms were performed using the TCGABiolinks package based on the TCGAanalyze_EAcomplete and TCGAvisualize_EAbarplot functions. The terms with enrichment significance p value lower than 0.05 were considered significantly enriched.

2.6. Molecular docking

Based on the above findings, the active ingredient with the most significant number of targets was selected as the ligand, and its targets with the largest node degree in the PPI network was chosen as the receptor to perform molecular docking. We downloaded three-dimensional structures of the active ingredients from PubChem CID. We obtained protein structures of the targets using the PDB database and imported them into AutoDockVina and MGLtools to perform molecular structure processing and molecular docking.

2.7. Animals

This study included ten-week-old female Sprague-Dawley rats weighing 175.7–221.4 g (n = 50), which were bought from Shanghai Laboratory Animal Center, Co. Ltd (Shanghai, China). The animals were kept in a 25 ± 2 °C environment with 56 ± 13 % humidity in standard cages and a dark/light cycle of 12 h. Food and Tap water were accessible to rats ad libitum. The acclimation time for the rats in the environment before subsequent experiments was one week. Approval for animal experiments was obtained from the ethics commission of Shanghai Traditional Chinese Medicine Hospital (Shanghai, China) (approval no. 20190103). The experimental protocols agreed with the Chinese Ministry of Science and Technology standards for the Care and Use of Laboratory Animals.

2.8. Establishment PCOS rat model and drug treatments

For investigating the effect of Bajitian-Danshen, fifty rats were divided into five groups, comprising the control, PCOS, PCOS + Baj-Dan Low, PCOS + Baj-Dan Medium, and PCOS + Baj-Dan High. The low-dose group received a range of 0.25 g/kg/day, the medium-dose group received a range of 0.5 g/kg/day, while the high-dose group received a range of 1 g/kg/day.

For investigating the effect of Tan-II, seventy rats were randomly distributed into seven groups of 10 rats in each group: 1) Control group containing rats intragastrically administered with saline for 21 days; 2) PCOS group, composed of PCOS rats intragastrically administered with saline for 21 days; 3) PCOS + PMA group, composed of PCOS rats that received an intragastric gavage of saline and an intraperitoneal administration of 500 μg/kg PMA daily for 21 days; 4) PCOS + Tan-IIA Low group, composed of PCOS rats that received an intragastrical administration of 25 mg/kg/day Tan-IIA for 21 days; 5) PCOS + Tan-IIA Medium group, composed of PCOS rats that received an intragastrical administration of 50 mg/kg/day Tan-IIA for 21 days; 6) PCOS + Tan-IIA High group, composed of PCOS rats that received an intragastrical administration of 100 mg/kg/day Tan-IIA for 21 days; and 7) PCOS + PMA + Tan-IIA High group, containing PCOS rats intraperitoneally receiving 500 μg/kg PMA/day and intragastrically administered with 100 mg/kg/day Tan-IIA for 21 days. Tan-IIA was dissolved in normal saline.

For PCOS rat model establishment, 60 rats were subjected to daily administration of HCG (3.0 IU/day) and two doses of INS subcutaneously for a period of 22 days. From the 1st to the 11th day, the dose of INS was gradually increased from 0.5 to 3.0 U/day; the dose of INS was kept at 3.0 U/day from day 12 to day 22. The 10 rats in the control group were subcutaneously administered with the same volume of normal saline two times/day for 22 days. The first days of the experiments, 5 % dextrose solution was given as drinking instead of the conventional drinking water. The weight of rats taken each week while vaginal smear was, monitored each day until the 23rd day. The establishment of the PCOS model was confirmed by the loss of rat normal estrous cycle.

2.9. Determination of body mass index (BMI), Lee's index, and ovarian quotiety

At the end of the experiment, the length of rats from the anus to the nose was detected and used for calculating BMI, Lee's index and ovarian quotiety using the following formulas: $\mathrm{Lee's\,index} = \frac{\sqrt[3]{BodyWeigth}}{Length} \times 1000$ (Gu et al., 2020); $\mathrm{BMI} = \frac{Weight}{Length^2}$; $\mathrm{Ovaries\,Quotiety} = \frac{OvarianWeigth}{BodyWeigth(mg/100g)}$ (Yu et al., 2014). The unit of length was cm and that of the weight was g.

2.10. Specimen collection

After being fasted overnight the last day of the experiment, the rats were subjected to sodium pentobarbitone (55 mg/kg) injection, intraperitoneally. Next, the abdominal aorta blood (5 ml) was collected and centrifuged (1,500 × g for 20 min at 4 °C) to obtain the serum. For the collection of ovarian tissue, the rats were killed by injection of high dose pentobarbital (250 mg/kg). The death was confirmed by exsanguination and the ovarian tissue was collected after dissection. For gene expression analysis, immediate immersion of the ovaries in liquid nitrogen was conducted to guarantee optimal preservation. For other experiments, the collected ovaries were immediately weighted and conserved in a − 80 °C fridge samples; before each experiment, the tissue was fixed in 4 % paraformaldehyde at 25 °C for 24 h.

2.11. ELISA detection of hormones and TNF-α levels

ELISA kits were used for detecting the levels of LH (Invitrogen, Shanghai, China), testosterone (Abcam, #ab108666), FSH (Invitrogen, Shanghai, China) and TNF-α (Abcam, #ab181421) in the serum following the manuals provided by the manufacturers. The levels were calculated based on the absorbance at 450 nm that was detected spectrophotometrically.

2.12. Histomorphometry analysis

The ovarian tissues fixed as described above were treated with gradient concentrations of ethanol (50, 70, 80, 90, and 100 %) for 30 sec and subsequently washed with xylene. The 4-μm thick sections were stained with picric acid for 30 min at room temperature and then with hematoxylin-eosin for 15 min at room temperature. Histomorphometry and histological examination of the tissues were performed using a microscope (Leica DM5000 fluorescence, Leica Microsystems, Inc.).

2.13. TUNEL assay

After deparaffinization with Histo-Clear, sections (6 μm thickness)

were permeabilized in 0.3 % Triton X-100. Apoptosis was then detected in the tissues using a specific TUNEL antibody, and the Dead-End™Colorimetric TUNEL System (Promega, Madison, USA) was used for detection according to the manufacturer's recommendations. Olympus IX81 microscope (Olympus America Inc., Center Valley, PA) was used for microscopic analysis, and green fluorescence was used to identify TUNEL-positive cells; diamidino-2-phenylindole (DAPI) counterstaining was used to identify cell nuclei.

2.14. Immunofluorescence staining

Deparaffinized ovarian sections (6 μm thickness) were mounted on coated glass slides and then washed with PBS (pH 7.4), followed by two rinses with PBS containing 0.5 % TritonX-100. After blocking in IgG-free 2 % bovine serum albumin (BSA sigma) for 30 min, the slides were incubated overnight at 4 °C with anti-p53 antibody [pAb122] (ABCAM, catalog number: ab90363, dilution 1:500) and anti-c-Fos antibody [2H2] (ABCAM, catalog number: ab208942, dilution 1:500). The following day, the slides were incubated with a secondary antibody (goat anti-rabbit FITC-labeled) (Vector Labs., CA, USA, FI −1000). Slides were counterstained with Vectashield containing DAPI (VectorLabs., CA, USA, H-1200). Sections of ovaries were observed and imaged using a digital camera (Nikon DS -U2, Japan) in conjunction with an Olympus BX51 fluorescence microscope.

2.15. Isolation and culture of granulosa cells (GCs) from rat ovaries

To isolate GCs, six immature (19–24 days old) female rats were given a subcutaneous injection of PMSG (150 IU/kg), and their ovaries were harvested after 48 h. Ovarian GCs were then isolated by follicular puncture (23) and pooled. After filtering the cells and centrifugation at $200 \times g$ at 4 °C for 5 min, the supernatant was removed. GCs were then used to prepare a cell suspension with Dulbecco's modified Eagles medium F12 (DMEM/F12 medium, Thermo Fisher Scientific, Inc.) containing 0.05 mg/ml gentamicin, selenium, transferrin, and INS. The isolated GCs were seeded into a 6-well cell culture plate (5×10^4 cells/ml) in DMEM/F12 medium and incubated in a 5 % CO_2 atmosphere at 37 °C for 24 h in a humidified atmosphere.

2.16. Cell transfection

FOS small interfering (si) RNA was used to knock down FOS expression in GCs. AllStars scrambled siRNA were employed as negative controls (NC-siRNA). The siRNA sequences were as follows: si-FOS#1, 5′- GACCTAGGGAGGACCTTATCT-3′; si-FOS#2, 5′-GGCAAAGTA-GAGCAGCTATCT-3′; and si-FOS#3, 5′- GACCTGTCTGGTTCCTTCTAT-3′. Lipofectamine® RNAiMAX (0.5 μl, 50 nM; Thermo Fisher Scientific, Inc.) was combined with siRNA (0.5 μl) for 20 min prior to experiments. GCs were cultured into a 6-well cell culture plate (3–5 × 104 cells/ml) until 90–95 % confluence; GCs were then assigned to the following groups: (i) normal, non-transfected cells; (ii) si-NC, transfected with NC-siRNA; (iii) si-FOS#1, transfected FOS siRNA-1; (iv) si-FOS#2, transfected with FOS siRNA-2; and (v) si-FOS#3, transfected with FOS siRNA-3. The next day, transfection efficiency was assessed by RT-qPCR and Western blotting.

2.17. Establishment of insulin resistance (IR) model of GCs and treatments

GCs were seeded in DMEM/F12 medium as described above. IR GCs were obtained by treating GCs with 1 μmol/L dexamethasone for three days. The culture medium was harvested to measure glucose levels using a commercial glucose and sucrose assay kit. GCs were allocated to five groups: i) Normal group, GCs without treatment; ii) IR group, INS-resistant GCs; iii) IR + NC group, IR-treated GCs that were transfected with si-NC; iv) IR + si-FOS, IR-treated GCs that were transfected with si-

FOS; and v) IR + Tan-IIA group, IR-treated GCs that were subjected to 200 nM Tan-IIA treatment.

2.18. Viability assay

After treatment, the viability of the cells in each group was assessed by performing the MTT assay. Cells (1×10^4 cells/well) were cultivated in 96-well plates for 48 h and subsequently added with 0.2 mg/ml MTT reagent (Sigma-Aldrich; Merck KGaA) for an additional 4 h incubation at 37 °C in 5 % CO_2. Later, formazan crystals were dissolved for 20 min using DMSO. Cell viability was gaged after detecting the absorbance at 490 nm using a microplate reader (Tecan Group, Ltd.).

2.19. RNA isolation and RT-qPCR

Total RNA from the GCs and rat ovary homogenates was isolated using the TRIzol® reagent and used for cDNA synthesis with GoScript™ Reverse Transcription System (Promega Corporation) for 60 min at 42 °C based on the protocol described by the manufacturer. SYBR-Green PCR master mix (Thermo Fisher Scientific, Inc.) was used for RT-qPCR amplification. Primer sequences were: PTGS2 forward: 5′- ACACTC-TATCACTGGCATCC-3′, reverse 5′-GAAGGGACACCCTTTCACAT-3′; GADPH forward: 5′- ACGGCAAGTTCAACGGCACAG-3′, reverse 5′-GAAGACGCCAGTAGACTCCACGAC-3′; c-Fos forward: 5′-AGCATGGGCTCCCCTGTCA-3′, reverse 5′- GAGACCAGAGTGGGCTGCA-3′; TP53 forward: 5′-CCACCTTCTTTGTCCTGCCTG-3′, reverse 5′-GTCGGCTCCGACTATACCACTATC-3′; c-Jun forward: 5′- ACCTTCAA-CACCCCAGCCATG-3′, reverse 5′- GGCCATCTCTTGCTCGAAGTC −3′; MMP9 forward: 5′- AGGTGCCTCGGATGGTTATCG-3′, reverse 5′-TGCTTGCCCAGGAAGACGAA-3′; CASP3 forward: 5′-GGTATTGAGACA-GACAGTGG-3′, reverse 5′- CATGGGATCTGTTTCTTTGC-3′. The thermal cycling conditions were activation at 50 °C, denaturation at 95 °C for 30 sec, 40 cycles of denaturation at 95 °C for 5 sec, and annealing at 60 °C for 30 sec. The $2^{-\Delta\Delta Cq}$ method was applied to quantify mRNA expression levels relative to GAPDH.

2.20. Western blot analysis

Cells and tissue homogenates were treated for 30 min with RIPA (cat. no. ab7937; Abcam). Next, after centrifugation (15 min, 11,500 × g, 4 °C), the BCA Protein Assay kit (cat. no. 23227; Thermo Fisher Scientific, Inc.) was employed for detecting total protein concentration. Protein (50 μg) was loaded for 12 % SDS-PAGE electrophoresis and transferred onto PVDF membranes. Afterwards, following blocking in 5 % at 25 °C for 2 h, the membranes were treated with primary antibodies against GAPDH (1:5,000; cat. no. ab8245; Abcam), anti-c-Fos antibody (1:1,000; cat. no. ab302667; Abcam), anti-PTGS2 antibody (1:1,000; cat. no. ab151571; Abcam), anti-c-Jun antibody (1:1,000; cat. no. ab40766; Abcam) and anti-p53 antibody (1:1,000; cat. no. ab90363; Abcam) overnight at 4 °C. Next, after washing with Tris-buffered saline added with 0.05 % Tween-20 (TBST), the membranes were treated for 1 h at 25 °C with the HRP-conjugated secondary antibody (1:5,000; cat. no. ab7097; Abcam). The ECL reagent (cat. no. WBKLS0050; EMD Millipore) was used for visualization, followed by densitometry analysis using the ImageJ software (version 1.47, National Institutes of Health).

2.21. Statistical analysis

One-way ANOVA followed by Bonferroni's post hoc test was used for detecting the statistical significance among three or more groups, while the T-test was used for analyzing the comparative difference among two groups using GraphPad Prism software version 8.0.1 (GraphPad Software, Inc.). $P < 0.05$ was considered for significant difference among groups.

3. Results

3.1. Identification of hub bioactive ingredients of Bajitian-Danshen pair and their potential target genes in PCOS treatment

A total of 83 active ingredients of Bajitian (18 ingredients) and Danshen (65 ingredients) were retrieved following the ADME screening criteria (OB > 30 %, DL > 0.18) (Additional File S1). The targets of each active ingredient were predicted in the TCMSP database, and 95 targets of the Bajitian-Danshen pair were obtained. After combining the lists of genes from GeneCards, OMIM, PharmGkb, DrugBank, and DisGeNET databases, a total of 2,205 PCOS-related genes were predicted. The Venn diagram intersection of the PCOS-related genes and the target genes of Bajitian-Danshen allowed the identification of 58 common genes as the targets of Bajitian and Danshen combination in the treatment of PCOS (Fig. 1A). Based on the list of ingredients targeting these 58 common genes, we identified 16 Bajitian ingredients and 44 Danshen ingredients as potentially effective ingredients against PCOS (Additional File S2). The PPI network of the 58 target genes of the Bajitian-Danshen pair in

PCOS treatment is depicted in Fig. 1B. The network comprised 57 connected nodes and 411 edges (Fig. 1B). The average number of neighbors was 14.421, with a diameter of 4 and a radius of 3 (Fig. 1B). MCODE analysis indicated the hub cluster of this PPI was composed of 21 genes (TP53, CASP3, PTGS2, MMP9, JUN, FOS, HSP90AA1, NFKBIA, CDKN1A, ESR1, PPARG, NOS3, GSK3B, CASP9, CDK2, TGFB1, PRKCA, EDN1, NOS2, AR, and PGR) as core genes in the PPI network (Fig. 1B). The functional enrichment analysis indicated that the target genes of the Bajitian-Danshen combination in PCOS were enriched in the biological processes of positive regulation of biosynthetic process (n = 13), positive regulation of nitrogen compound metabolic process (n = 11), positive regulation of apoptosis (n = 9), and positive regulation of programmed cell death (n = 9) (Fig. 1C). The most enriched cellular component terms were cell fraction (n = 10), neuron projection (n = 6), cell projection (n = 6), cell soma (n = 4), dendrite (n = 4), and integral to plasma membrane (n = 9), while the most enriched terms in the category of molecular function were adrenoceptor activity (n = 4), amine receptor activity (n = 5), alpha1 − adrenergic receptor activity (n = 3), and alpha − adrenergic receptor activity (n = 3) (Fig. 1C). The most
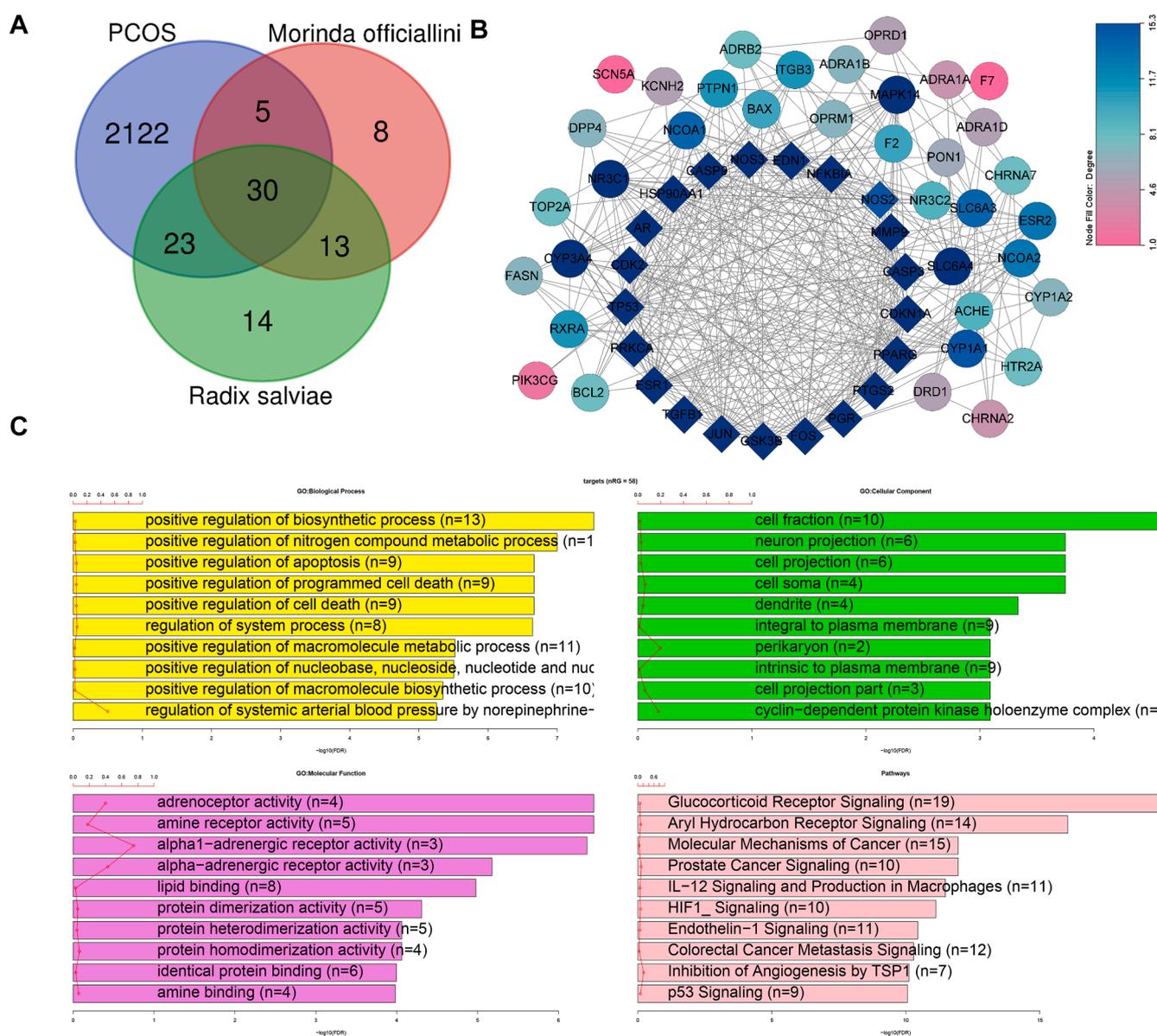

Fig. 1. Identification of active ingredients of Bajitian and Danshen in PCOS treatment and the functional roles of their targets. A- Venn diagram indicating the intersection of PCOS-related genes and targets of Bajitian and Danshen. B- Protein-protein interaction network of targets of Bajitian and Danshen ingredients in PCOS treatment. C- Functional enrichment of targets of Bajitian and Danshen ingredients in PCOS treatment.

important pathways potentially targeted by the Bajitian-Danshen ingredients in PCOS were Glucocorticoid Receptor Signaling (n = 19), Aryl Hydrocarbon Receptor Signaling (n = 14), molecular mechanisms of cancer (n = 15), Prostate Cancer Signaling (n = 10), IL-12 signaling and production of macrophages (11), and HIF1_Signaling (n = 10) (Fig. 1C). The ingredient-target network of the Bajitian-Danshen combination in PCOS treatment was generated and visualized using the CytoScape software (Fig. 2). The ingredient-target PPI network indicated Tan-IIA as

the hub component of the Bajitian-Danshen combination in PCOS treatment (MOL007154, degree 27, betweenness centrality 0.2070204172530126, closeness centrality 0.45703124999999994) followed by beta-sitosterol (MOL000358, degree 24, betweenness centrality 0.15759452247335504, closeness centrality 0.46062992125984253), dihydrotanshinlactone (MOL007100, degree 24, betweenness centrality 0.04483259476537794, closeness centrality 0.45348837209302323), 1,2,5,6-tetrahydrotanshinone (MOL001601,
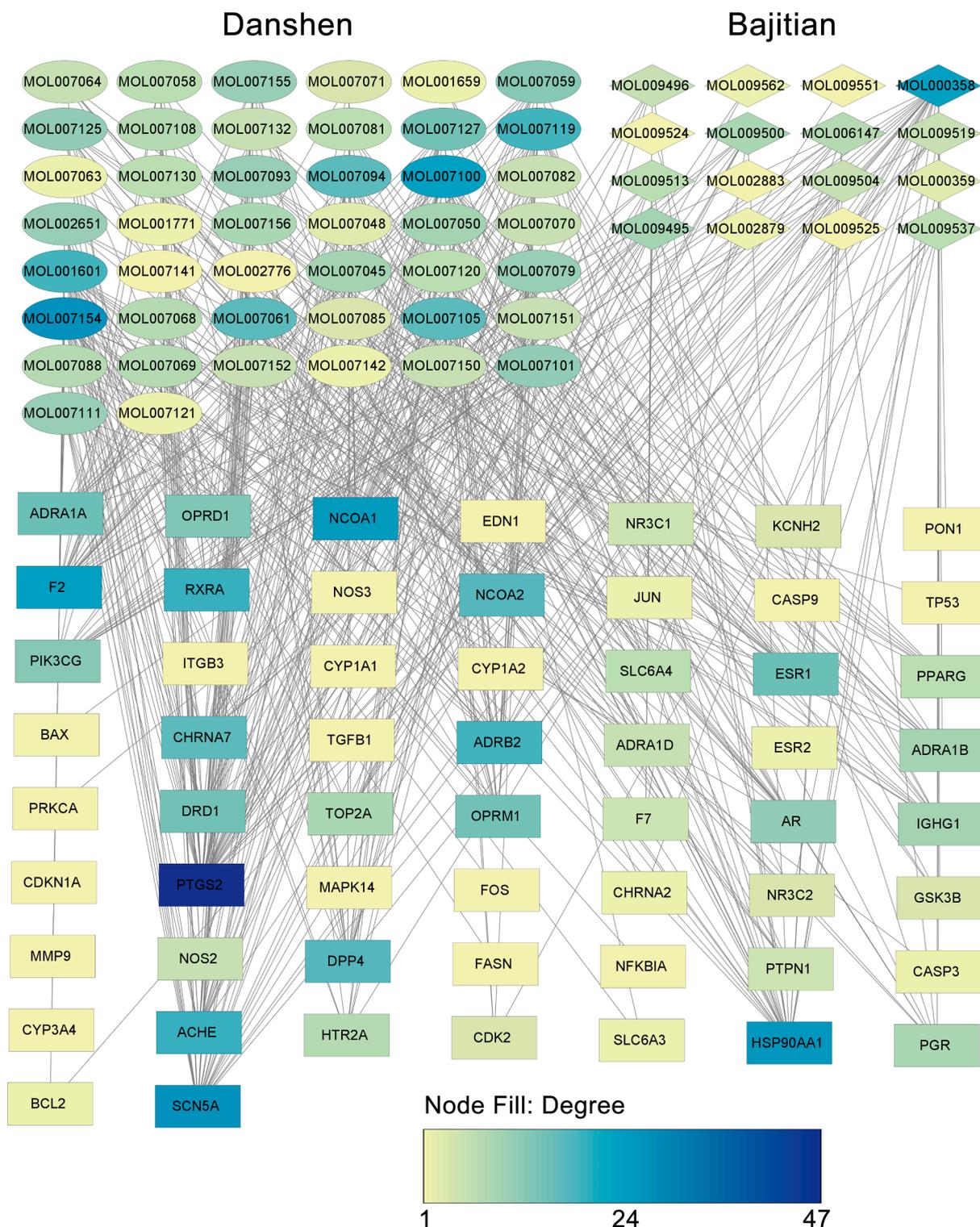

Fig. 2. Ingredient-gene interaction network. The ingredients of Bajitian and Danshen and their target genes were used for constructing the drug-gene interaction network.

degree 19, betweenness centrality 0.04779521728839308, closeness centrality 0.43333333333333335) that were also active in treating PCOS (Fig. 2). The node table indicating the network parameters was depicted in Additional File S3.

3.2. Protein-protein interaction network of Tan-IIA targets in PCOS and their functional enrichment analysis

Since Tan-IIA was found to be the ingredient with the highest number of targets in the treatment of PCOS, the 27 targets of this ingredient were used for protein–protein interaction network construction in the STRING database (Fig. 3A). The PPI network comprised 25 nodes and 78 edges with an average number of neighbors of 6.240 (Fig. 3A). The PPI network was imported into Cytoscape to identify the core targets and possible protein functional modules. Important targets of Tan-IIA were TP53, FOS, PTGS2, CASP3, MMP9, EDN1, NFKBIA, and JUN (Fig. 3A). These 27 Tan-IIA target genes were involved in the biological processes of positive regulation of the biosynthetic process (n = 8), drug metabolic process (n = 3), and homeostatic process (n = 6) (Fig. 3B). The prevalent cellular component terms were cell fraction (n = 7), microsome (n = 3), and vesicular fraction (n = 3) (Fig. 3B). The

most enriched molecular function terms were vitamin D 24-hydroxylase activity (n = 2), oxidoreductase activity acting on paired donors (n = 5), peptide binding (n = 4), and oxygen binding (n = 3) (Fig. 3B). The most enriched target pathways of Tan-IIA target genes in PCOS were Aryl Hydrocarbon Receptor Signaling (n = 7), Glucocorticoid Receptor Signaling (n = 8), PPAR Signaling (n = 6), MIF Regulation of Innate Immunity (n = 5), Small Cell Lung Cancer Signaling (n = 5), inhibition of angiogenesis by TSP1 (n = 4), ILK Signaling (n = 6), IL-8 Signaling (n = 6), HIF1_signaling (n = 5), and molecular mechanisms of cancer (n = 7) (Fig. 3B).

3.3. Molecular docking analysis

To find the critical genes that Tan-IIA could target, we performed subsequent clustering of the PPI network of Tan-IIA targets to identify the different groups of interactive proteins using the clustering option in the STRING database. We found a set of 10 genes (CASP3, BCL2, DPP4, MMP9, TP53, PTGS2, CDKN1A, NFKBIA, FOS, and JUN) as credible targets of Tan-IIA targets in PCOS treatment (Fig. 4A). As shown in Fig. 4A, JUN and FOS were identified to pertain to the first cluster, CASP3, DPP4, BCL2, TP53, PTGS2, CDKN1A, and NFKBIA belonged to
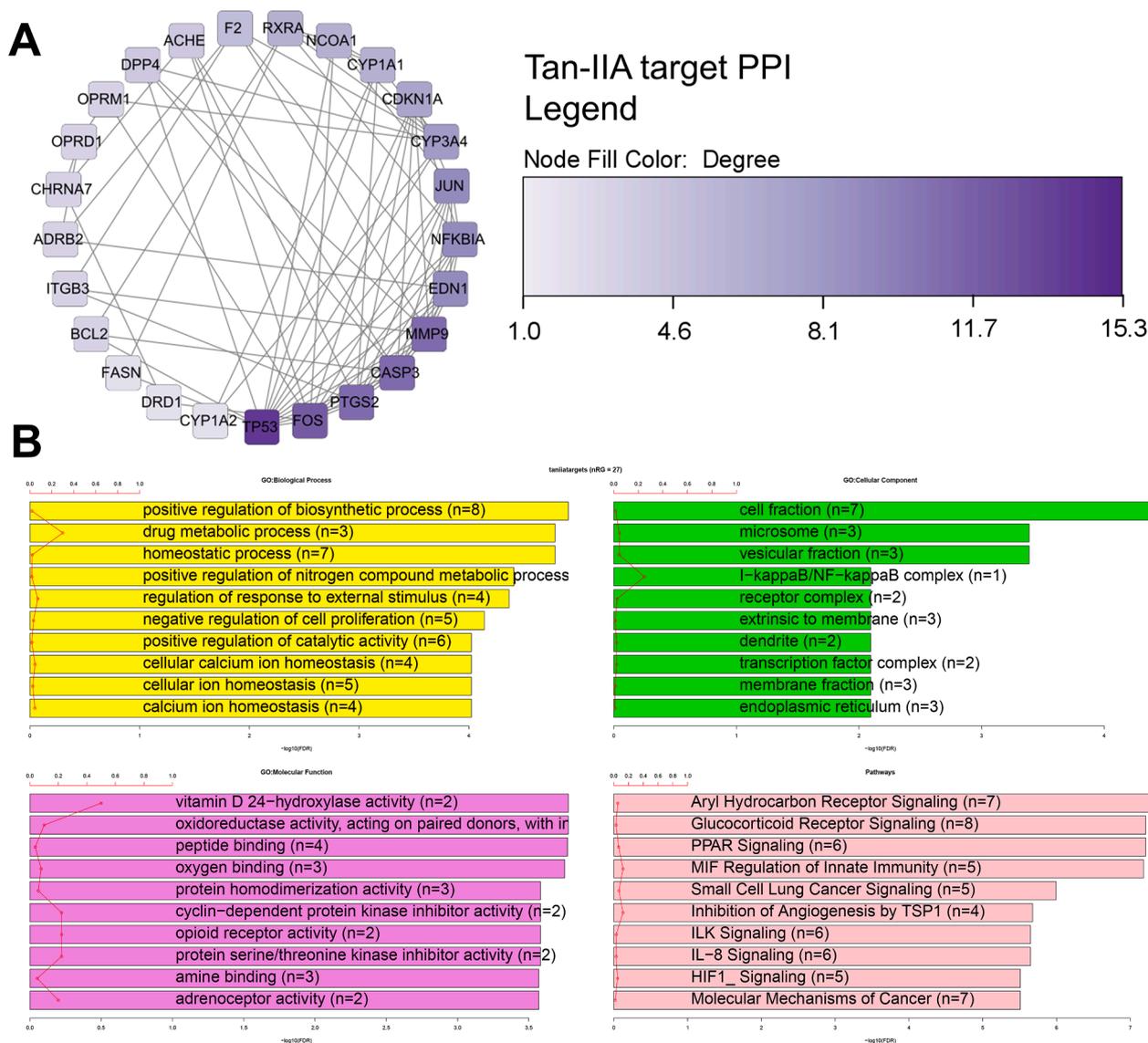

Fig. 3. Tan-IIA targets in PCOS treatment. A-Protein-Protein interaction network of Tan-IIA targets in PCOS treatment. Functional enrichment analysis of Tan-IIA targets in PCOS treatment. Tan-IIA = tanshinone IIA.
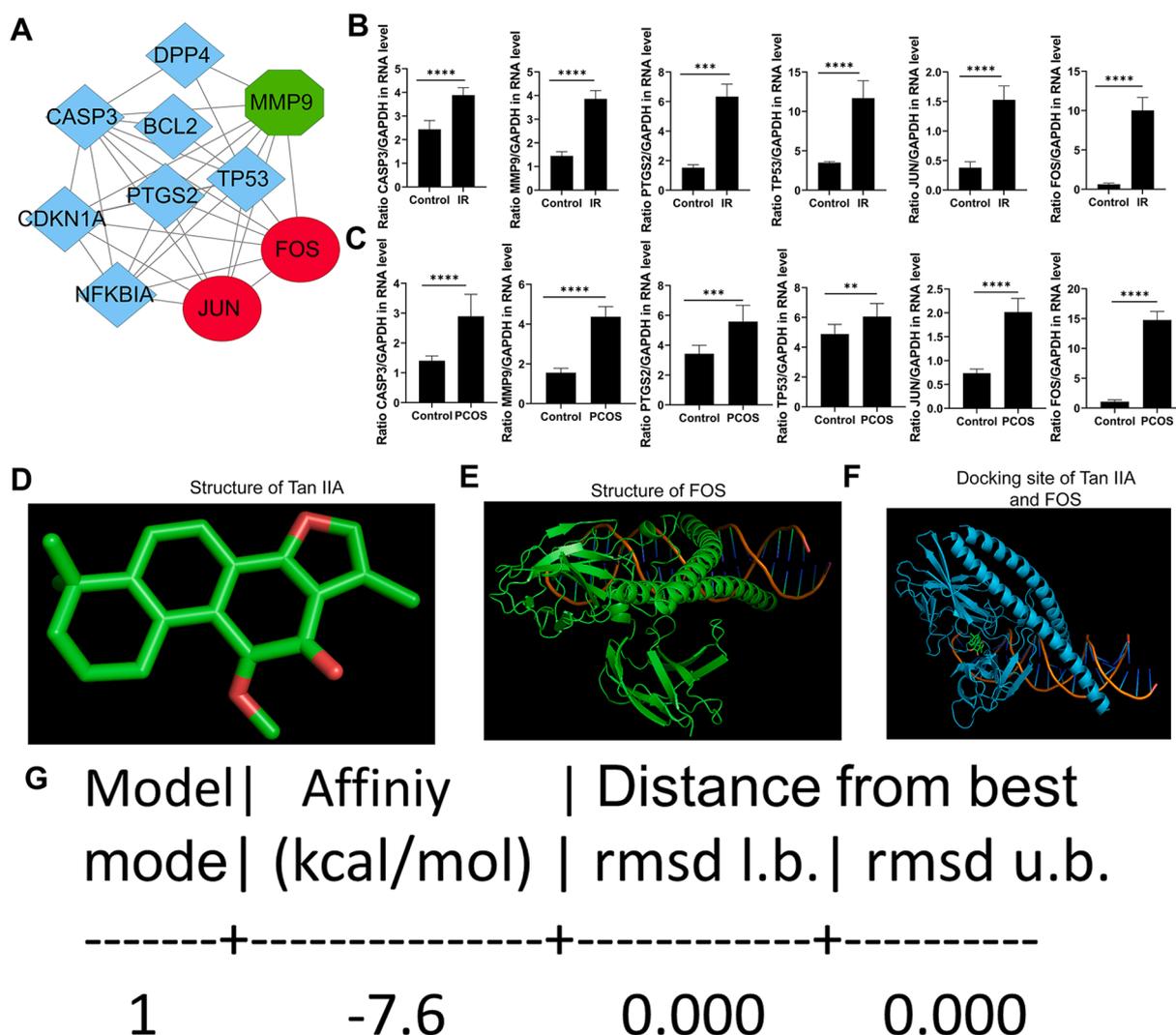
Fig. 4. Identification of key Tan-IIA targets in PCOS treatment. A- Hub clusters of key Tan-IIA targets in PCOS treatment obtained from the protein–protein interaction network. B- RT-qPCR validation of the mRNA expression of key Tan-IIA targets in PCOS treatment in IR GCs. C- RT-qPCR validation of the mRNA expression of key Tan-IIA targets in PCOS treatment in ovaries of PCOS rats. D- Molecular structure of Tan-IIA. D- Tridimensional structure of FOS. F-Docking of Tan-IIA and FOS. G- Binding affinity of Tan-IIA to FOS. Data are presented as the mean ± SEM. **$P < 0.01$, ***$P < 0.001$, ****$P < 0.0001$ vs. Control, Tan-IIA = tanshinone IIA, IR = Insulin-resistant, GCs = granulosa cells.

the second cluster, while MMP9 belonged to the third cluster. Thus, we subsequently verified the expression trends of CASP3, MMP9, TP53, PTGS2, FOS, and JUN in IR GCs and PCOS rat ovaries by RT-qPCR. As indicated in Fig. 4B and 4C, the expression levels of these genes were increased in IR GCs and PCOS rat ovaries, which indicated their roles in PCOS and the potential of Tan-IIA to revert their deleterious outcomes in PCOS.

Furthermore, we performed molecular docking and found that Tan-IIA (Fig. 4D) docked well to FOS (Fig. 4E) through several interactions with amino acid residues, as shown in Fig. 4F. The binding affinity between both molecules was −7.6 (Fig. 4G), indicating FOS is the most crucial target of Tan-IIA in PCOS.

3.4. Bajitian-danshen decoction counteracts PCOS and regulated predicted hub target genes

To explore the impact of the Bajitian-Danshen decoction on PCOS, PCOS rats were treated with low (PCOS + Baj-Dan Low), medium (PCOS + Baj-Dan Medium), and high (PCOS + Baj-Dan High) doses of the decoction. The results indicated that the Bajitian-Danshen decoction dose-dependently decreased PCOS-induced body weight gain (Fig. 5A),

ovarian weight (Fig. 5B), and ovarian quotiety (Fig. 5C). Additionally, the decoction significantly decreased PCOS-induced increase in BMI (Fig. 5D), Lee's index (Fig. 5E), LH (Fig. 5F), FSH (Fig. 5G), testosterone (Fig. 5H), and TNF-α (Fig. 5I). Furthermore, the results of HE staining showed that the control group had normal ovarian tissue morphology with various stages of follicles and multiple corpora lutea visible (Fig. 5J). On the other hand, the PCOS group exhibited numerous cystic expanded follicles and a significant decrease in the number of granulosa cells (Fig. 5J). After administering the Bajitian-Danshen decoction at different concentrations, there was a notable improvement in ovarian tissue morphology, with the high dose showing the most pronounced effects (Fig. 5J). The findings suggest that the herbal formulation can improve ovarian morphology, increase the number of ovarian granulosa cells, reduce the proliferation of follicle membrane cells and interstitial cells, and promote follicular development and ovulation (Fig. 5J). Moreover, we examined the effect of the Bajitian-Danshen decoction on the gene expression of the predicted hub targets, and the results indicated that the decoction dose-dependently counteracted PCOS-induced upregulations of CASP3, MMP9, TP53, PTGS2, FOS, and JUN (Fig. 5K). These results indicated that the Bajitian-Danshen decoction is effective in treating PCOS, and its effect might be driven by regulating
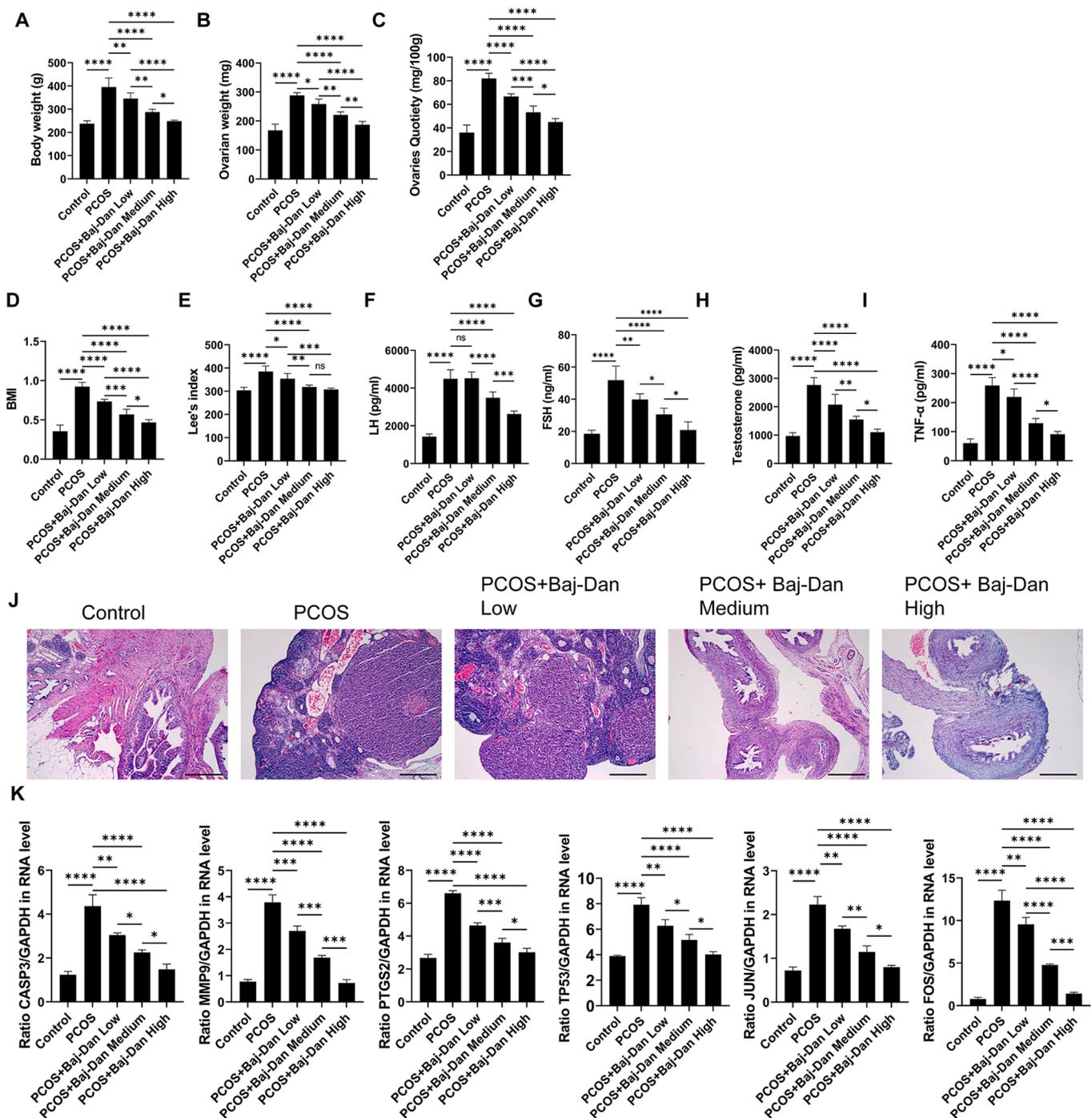
Fig. 5. Effects of Bajitian-Danshen decoction on (A) body weight, (B) weight of ovaries, (C) ovarian index, (D) BMI, (E) Lee's index, (F) LH, (G) FSH, (H) testosterone, (I) TNF-α, (J) Ovary histopathological changes in rats with PCOS, and (K) the expression of CASP3, MMP9, TP53, PTGS2, FOS, and JUN. Data are presented as the mean ± SEM. *$P < 0.05$, **$P < 0.01$, ***$P < 0.001$, ****$P < 0.0001$ among the compared groups, ns = non-significant. Scale bar = 100 μm. Baj-Dan = Bajitian-Danshen.

the predicted targets.

3.5. The therapy activity of Tan-IIA on PCOS might be driven via regulating FOS

To investigate the effect of Tan-IIA on the expression of FOS, the immunofluorescence assay was performed on the ovary tissue of rats in the different groups (Fig. 6). The positive ratio of FOS in the PCOS and PCOS + PMA groups was significantly increased compared to the control group (Fig. 6). Nevertheless, after Tan-IIA treatment, the positive ratio

of FOS was significantly and dose-dependently decreased in the PCOS rats (Fig. 6). In addition, Tan-IIA significantly abolished the effect of PMA on the FOS-positive ratio in the PCOS rats (Fig. 6). These results indicated that the therapy activity of Tan-IIA on PCOS might be driven via regulating FOS.

3.6. Tan-IIA counteracts deleterious effects in rats with PCOS via FOS/JUN/TP53 signaling

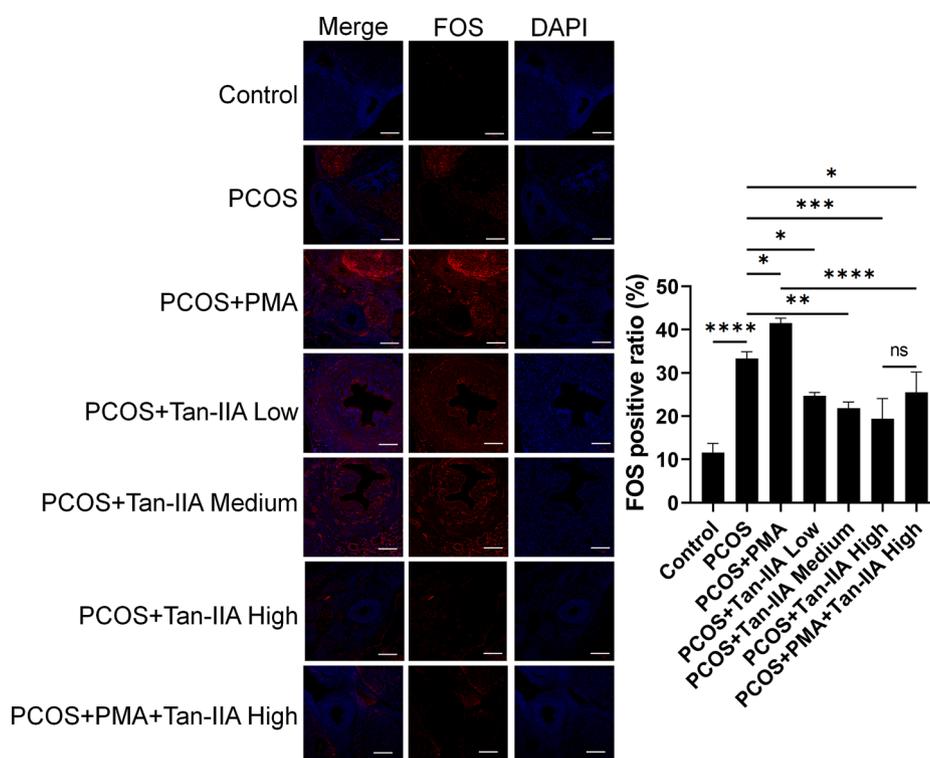In order to experimentally validate the therapeutic effect of Tan-IIA

Fig. 6. Effect of Tan-IIA on FOS expression in PCOS rats. Immunofluorescence analysis of FOS in the ovary tissues of rats subjected to different treatments. Data are presented as the mean ± SEM. *P < 0.05, **P < 0.01, ***P < 0.001, ****P < 0.0001 among the compared groups, ns = non-significant, Tan-IIA = tanshinone IIA. Scale bar = 50 μm.

on PCOS and its potential regulation of FOS, a rat model of PCOS was established and treated with PMA, Tan-IIA at different doses, or the combined treatment of PMA and Tan-IIA. Compared to control rats, the weight of rats with PCOS was significantly increased (Fig. 7A). The body weights of rats in PCOS + Tan-IIA were dose-dependently decreased compared to the PCOS group (Fig. 7A). Moreover, treatment with PMA further increased the body weights of PCOS rats, but this effect was abolished by the treatment with a high dose of Tan-IIA (Fig. 7A). The weights of the ovaries of rats in the PCOS rats were significantly increased compared to control rats, and this effect was further increased by the treatment with PMA (Fig. 7B). On the contrary, the treatment of PCOS rats with Tan-IIA significantly decreased the ovarian weight in a dose-dependent manner (Fig. 7B). Moreover, the ovarian weights of rats were notably reduced in the PCOS + PMA + Tan-IIA High group compared to the PCOS + PMA group rats (Fig. 7B). Additionally, the quotiety of ovaries in the PCOS was remarkably increased comparatively to the control group, which was further promoted in the PCOS + PMA groups (Fig. 7C). However, compared to the PCOS groups, Tan-IIA decreased ovarian quotiety dose-dependently (Fig. 7C). In addition, as shown in Fig. 7D and 7E, BMI and Lee's index were all increased in PCOS and this effect was further promoted by PMA treatment. Nonetheless, Tan-IIA dose-dependently decreased BMI and Lee's index, and abrogated the effect of PMA on these variables (Fig. 7D and 7E). The effect of Tan-IIA on the serum levels of TNF-α, testosterone, LH, and FSH was investigated. The results indicated that the serum levels of TNF-α, testosterone, LH, and FSH in the PCOS group were remarkably increased compared to the control group (Fig. 7F-7I). Furthermore, TNF-α, LH, FSH, and testosterone levels in the PCOS rats treated with different doses of Tan-IIA were significantly decreased compared to the PCOS group (Fig. 7F-7I). Moreover, in the PCOS + PMA + Tan-IIA group, FSH, LH, TNF-α and testosterone levels were obviously diminished compared to the PCOS + PMA group (Fig. 7F-7I). To investigate whether the action of Tan-IIA on the histopathological changes of PCOS rats, the HE staining of ovary tissue from rats in different groups was performed (Fig. 7J). The

microscopic images indicated that the follicles and corpora lutea in the ovaries of rats in the control group were in primordial follicles, primary follicles, and secondary follicles developmental stages (Fig. 7J). Serious histopathological changes were recorded in the PCOS and PCOS + PMA rats (Fig. 7J). Moreover, compared to the control rats, the number of large cystic follicles filled with fluid substantially increased while the GC layers deteriorated in the PCOS and PCOS + PMA groups (Fig. 7J). Moreover, a decreased number of corpora lutea was observed in both the PCOS and PCOS + PMA rats compared to the control rats (Fig. 7J). Treatment of PCOS rats with Tan-IIA at different doses obviously alleviated the pathological changes observed in the PCOS rats. In the PCOS + PMA + Tan-IIA treatment group, the pathological changes in ovarian tissue observed in the PCOS and PCOS + PMA rats were abrogated, with an increased number of GC layers and a decreased number of cystic follicles (Fig. 7J). These results indicated that Tan-IIA counteracts the pathological changes of ovaries and might regulate deleterious effects of PCOS, especially inflammation and hormonal disorders in PCOS, via regulating FOS.

3.7. Effect of Tan-IIA on cell apoptosis in vivo

We sought to verify the effect of Tan-IIA on cell apoptosis *in vivo*. The Tunel assay was performed on ovarian tissue sections. The results displayed that, compared to the control group, the level of apoptosis in the PCOS rats was significantly increased (Fig. 8). In addition, treatment with PMA promoted this effect (Fig. 8). Nevertheless, treatments of PCOS rats with various doses of Tan-IIA led to a significantly reduced level of apoptosis in the ovarian tissue compared to the PCOS group (Fig. 8). Furthermore, a high dose of Tan-IIA abolished the effect of PMA, as indicated in the PCOS + PMA group.
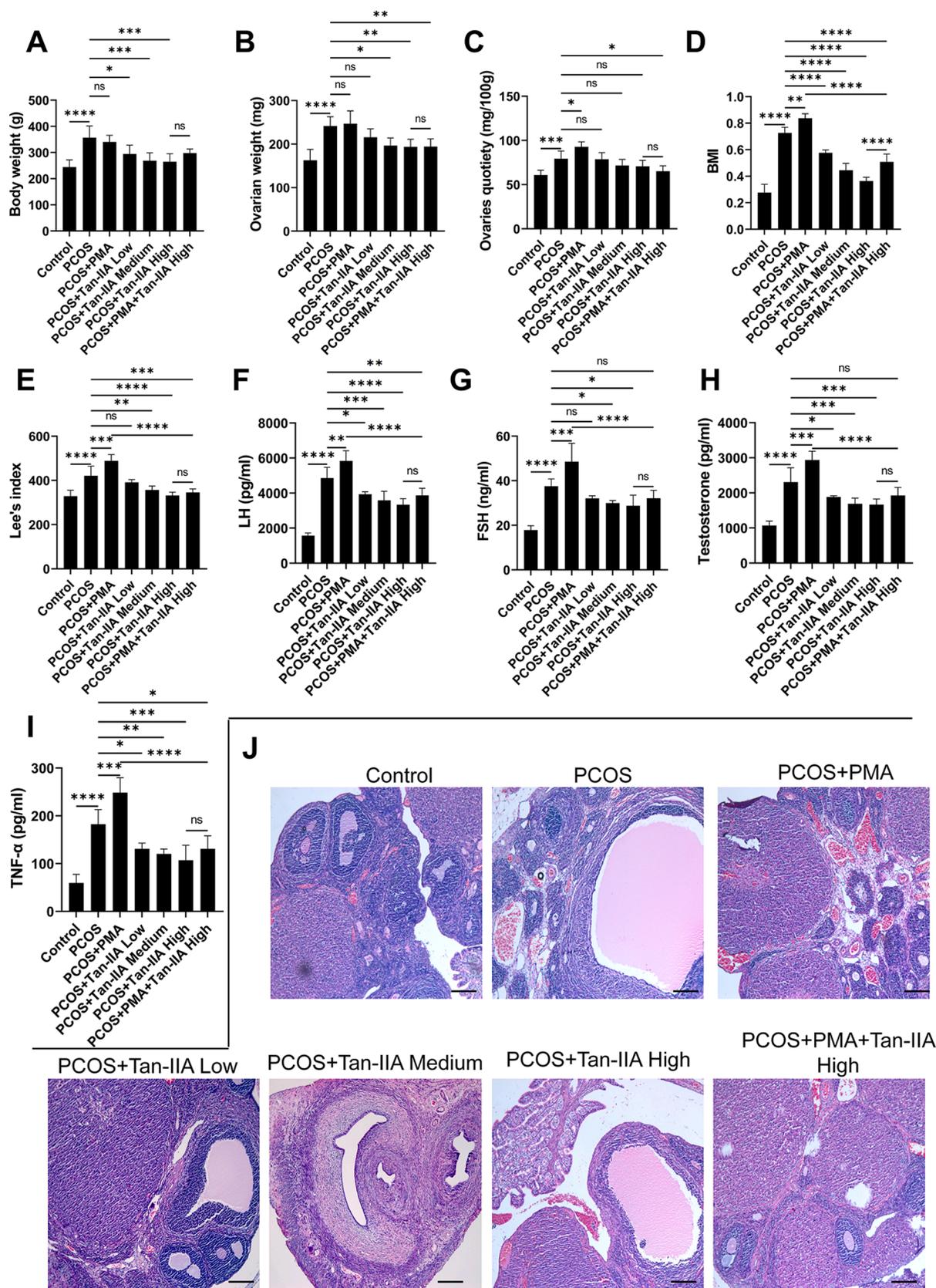
Fig. 7. Effects of Tan-IIA and PMA on (A) body weight, (B) weight of ovaries, (C) quotiety of ovaries, (D) BMI, (E) Lee's index, (F) LH, (G) FSH, (H) Testosterone, (I) TNF-α, and (J) Ovary histopathological changes in rats with PCOS. Data are presented as the mean ± SEM. *P < 0.05, **P < 0.01, ***P < 0.001, ****P < 0.0001 among the compared groups, ns = non-significant, Tan-IIA = tanshinone IIA. Scale bar = 100 μm.
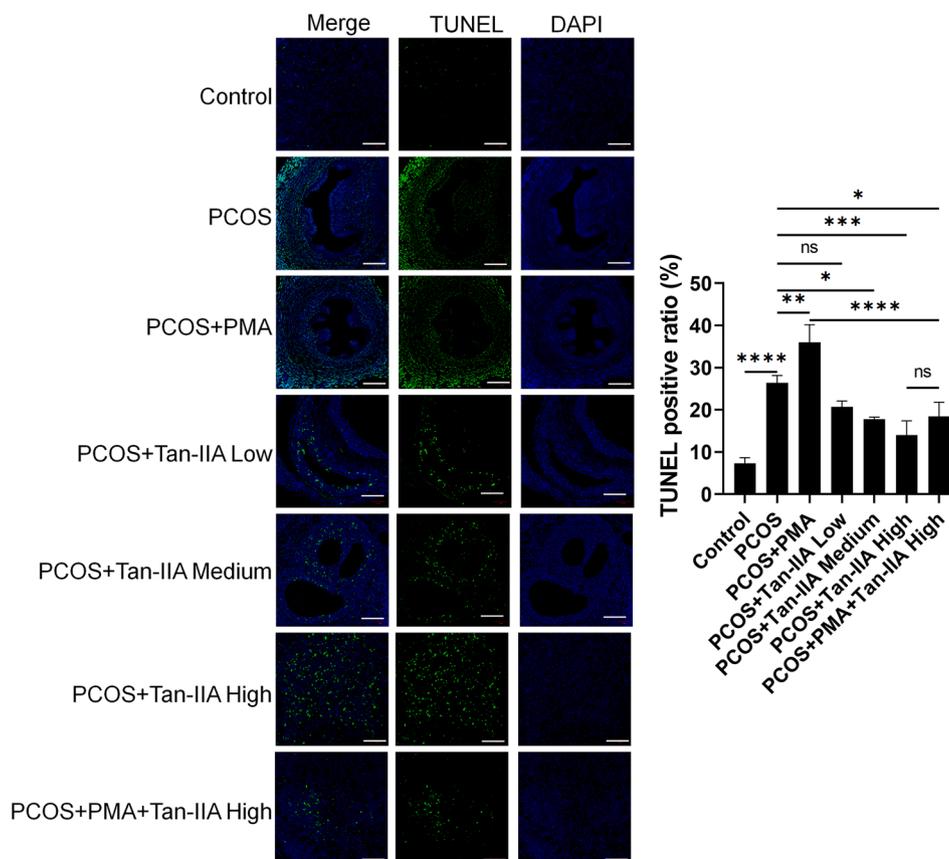
Fig. 8. Effect of Tan-IIA on apoptosis in PCOS rats. Tunel immunostaining analysis of FOS in the ovary tissues of rats subjected to different treatments. *P < 0.05, **P < 0.01, ***P < 0.001, ****P < 0.0001 among the compared groups. ns = non-significant, Tan-IIA = tanshinone IIA. Scale bar = 50 μm.

3.8. Tan-IIA regulate the expression of TP53, PTGS2 and JUN in the ovarian tissues via FOS

The TP53, PTGS2 and JUN expression levels were detected by RT-qPCR (Fig. 9A) and western blotting (Fig. 9B). The results indicated that the TP53, PTGS2 and JUN expression levels in the PCOS and the PCOS + PMA groups were notably increased compared to the normal group (Fig. 9A and B). Furthermore, the TP53, PTGS2 and JUN expression in the PCOS + PMA + Tan-IIA High group was notably decreased comparatively to the PCOS + PMA group (Fig. 9A and B). Furthermore, immunofluorescence staining of TP53 indicated that the TP53-positive ratio was increased in the PCOS group (Fig. 9C). PMA treatment of PCOS rats further promoted the TP53-positive ratio (Fig. 9C). The positive ratio of TP53 was decreased by high-dose Tan-IIA treatment in comparison with the PCOS and PCOS + PMA groups (Fig. 9C). These results indicated that Tan-IIA regulates the expression level of TP53, PTGS2, and JUN via targeting FOS.

3.9. Tan-IIA inhibits the proliferation and regulates FOS, TP53, PTGS2, and JUN in IR-treated GCs

To investigate the effect of Tan-IIA on GCs, these cells were transfected with three si-RNAs targeting FOS, and FOS mRNA and protein expression levels were analyzed by RT-qPCR and western blotting. Relatively to si-NC and untransfected cells, protein expression of FOS in the si-FOS#1, si-FOS#2, and si-FOS#3 groups was notably reduced, particularly in the si-FOS#2 group (Fig. 10A and B). Therefore, the FOS siRNA-2 was transfected in the GCs, and cell viability in different groups was determined by MTT assay (Fig. 10C). Cell viability in the IR and IR + si-NC groups was notably reduced compared to the normal group (Fig. 10C). The viability of IR-GCs treated with Tan-IIA or transfected

with si-FOS was higher relative to untreated cells (Fig. 10C). In addition, TNF-α (Fig. 10D) and FOS (Fig. 10E) levels in the serum of IR and IR + si-NC rats were notably increased relative to the normal group. In addition, relative to the IR group, TNF-α and FOS levels in the IR + si-FOS and IR + Tan-IIA groups were notably reduced (Fig. 10D and 10E). These results suggested that Tan-IIA improved the viability of IR-GCs by regulating the production of FOS.

TP53, PTGS2, and JUN expression levels were analyzed using RT-qPCR (Fig. 10F) and western blotting (Fig. 10G). The expression of TP53, PTGS2, and JUN in the IR and IR + si-NC groups were notably augmented relative to the normal group (Fig. 10F and G). Furthermore, TP53, PTGS2 and JUN expression levels in both IR + si-FOS and IR + Tan-IIA groups were notably lower relatively to the IR group (Fig. 10F and G). The effect of Tan-IIA treatment on FOS, TP53, PTGS2, and JUN expression levels was also notably greater relative to si-FOS transfection (Fig. 10F and G). These results indicated that Tan-IIA treatment downregulated the expression of FOS, TP53, PTGS2, and JUN.

4. Discussion

PCOS is a severe condition encountered in women. Up to date, the prophylactic and therapeutic options for PCOS are limited, which necessitates the uncovering and validation of novel alternative drugs for this disease. Previous studies have indicated the potential of the traditional Chinese medicine herbs Bajitian and Danshen and some of their components in the treatment of PCOS. However, the molecular mechanism of Bajitian and Danshen in the treatment is still ill-defined. In the present study, we aimed to identify the key ingredient of Bajitian and Danshen in the treatment via network pharmacology and explore the molecular mechanism underlying its mode of action. We identified 60 active ingredients in Bajitian and Danshen that could target 58 genes
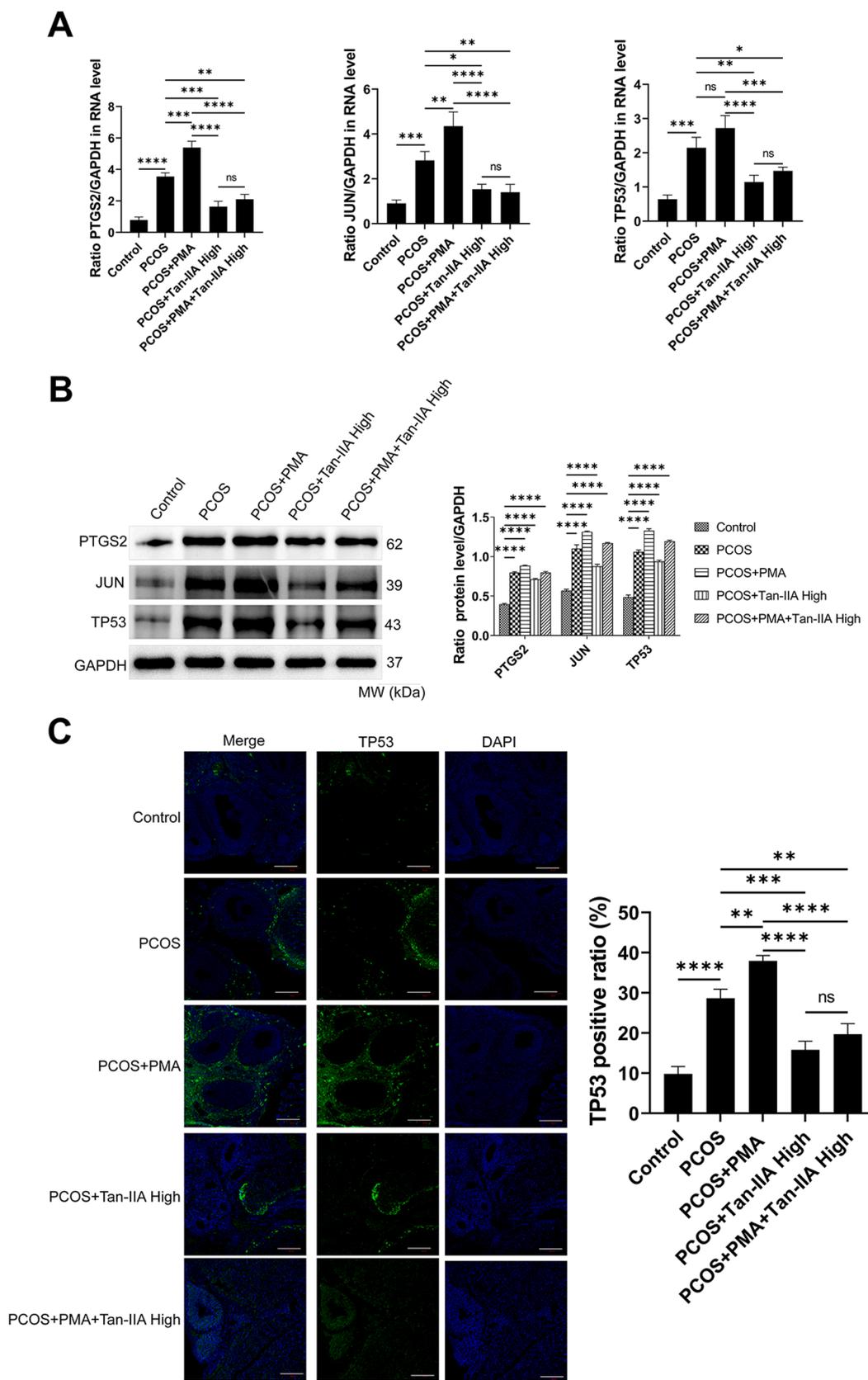
Fig. 9. Effect of Tan-IIA on the FOS/JUN/TP53 signaling pathway. A- RT-qPCR detection of FOS, JUN, and TP53 in different treatment groups. B- Western blot detection of FOS, JUN, and TP53 in different treatment groups. *P < 0.05, **P < 0.01, ***P < 0.001, ****P < 0.0001 among the compared groups. ns = non-significant, Tan-IIA = tanshinone IIA. Scale bar = 100 μm.
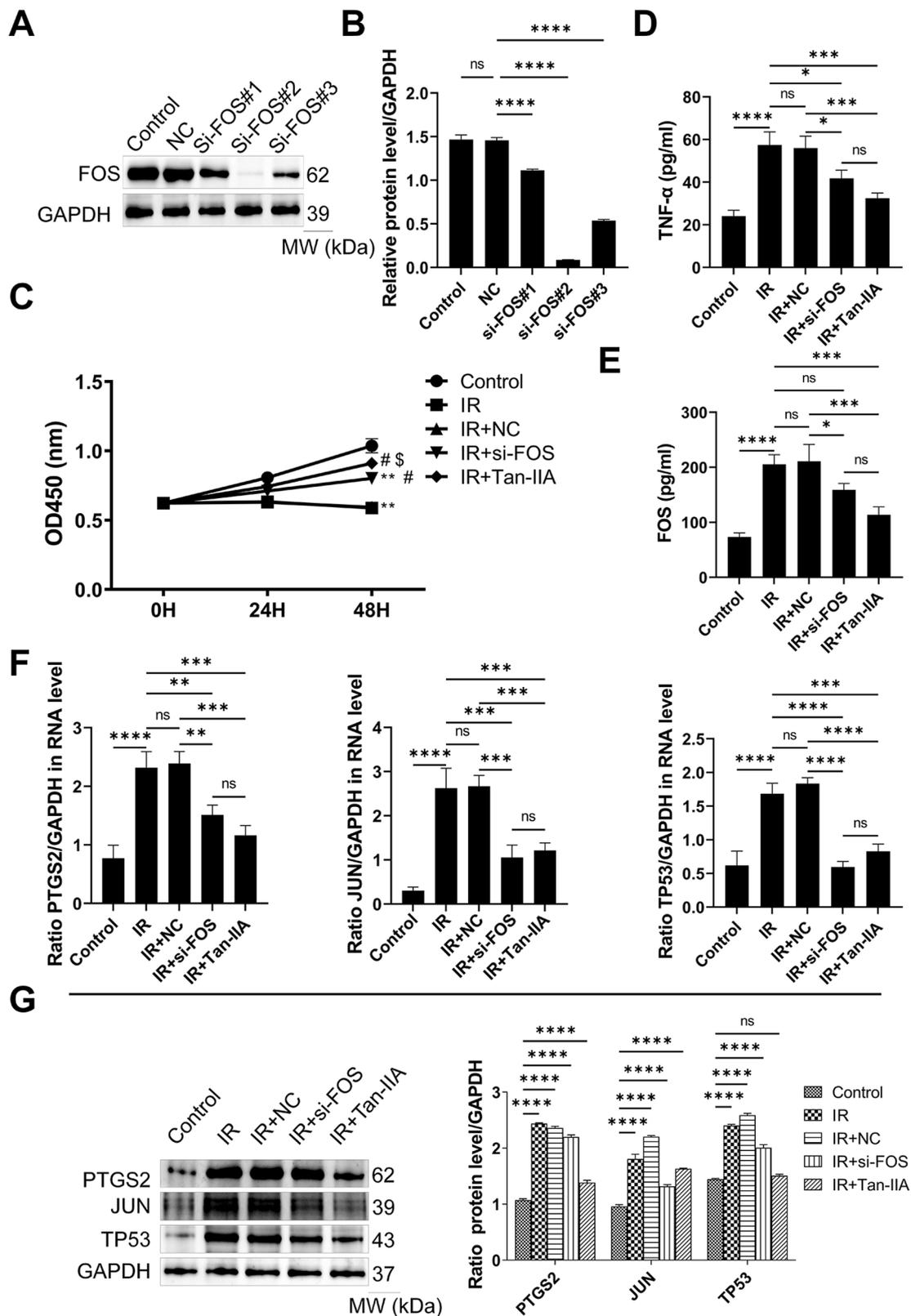
Fig. 10. Tan-IIA regulates the viability of IR GCs via the FOS/JUN/TP53 axis. A- Western blotting confirmation of FOS silencing in GCs. B- Densitometry analysis of western blot band from the confirmation experiments. C- Effect of Tan-IIA on the viability of IR GCs. D- ELISA analysis of TNF-α. E- ELISA analysis of FOS. F- RT-qPCR analysis of the expression FOS, JUN and TP53 in different treatment groups. G- Western blot analysis of the expression FOS, JUN and TP53 in different treatment groups. *P < 0.05, **P < 0.01, ***P < 0.001, ****P < 0.0001 among the compared groups or compared to control group, #P < 0.05 compared to IR, $P < 0.05 compared to IR + si-FOS, ns = non-significant, Tan-IIA = tanshinone IIA, IR = insulin-resistant, GCs = granulosa cells.

actively involved in the pathogenesis of PCOS. Among the identified ingredients, Tan-IIA was found to be the ingredient with the most targets (27 targets) in PCOS treatment, indicating that Tan-IIA is the hub ingredient of the Bajitian-Danshen combination for the treatment of PCOS. The 27 targets of Tan-IIA were involved in biological processes of muscarinic acetylcholine receptor signaling pathway, positive regulation of catalytic activity, positive regulation of the biosynthetic process, and homeostatic process, and the pathways of G − Protein Coupled Receptor Signaling, Aryl Hydrocarbon Receptor Signaling, MIF Regulation of Innate Immunity, and cAMP − mediated signaling. The PPI network based on the 41 targets of Tan-IIA indicated that these proteins constituted a strong regulatory module with PTGS2, JUN, FOS, TP53, PTGS2, and CASP3 as the hub genes. Molecular docking confirmed the interaction of Tan-IIA with FOS. To experimentally verify whether FOS was involved in the mode of action of Tan-IIA, a rat model of PCOS was established. The result indicated that FOS was upregulated in PCOS and that the activation of FOS by PMA promoted the deleterious effect of PCOS. In addition, the treatment with PCOS or PCOS + PMA rats with Tan-IIA inhibited the deleterious effect of PCOS and the activation of FOS. In addition, JUN and TP53 were all upregulated in PCOS and further promoted by the FOS activator PMA; however, the Tan-IIA reverted these expression trends. In addition, Tan-IIA alleviated IR-induced damage of GCs. Our study is the first to demonstrate that Tan-IIA alleviates the deleterious effect of PCOS by targeting the FOS/JUN/TP53 axis. These findings shed light on the molecular mechanism of PCOS and proposed Tan-IIA as a potential therapeutic.

Previous studies have indicated that Danshen has various bioactive properties. It was reported to exert hepatoprotective effect (Hong et al., 2017). It was found as a therapeutic drug for various diseases and conditions such as non-alcoholic fatty liver disease (Liu et al., 2022c), bowel disease, Alzheimer's Disease (Li et al., 2022b), coronary heart disease (Zhang et al., 2019), diabetic retinopathy (Piao et al., 2019), heart failure (Wang et al., 2020b), hepatic fibrosis (Cao et al., 2022), epilepsy (Huang et al., 2022), tumors such as breast cancer (Lin et al., 2019) and ovarian cancer (Qin et al., 2022), cerebral ischemia–reperfusion (Wan et al., 2021). Other studies have indicated that some ingredients, such as cryptotanshinone and tanshinone from Danshen, can alleviate the deleterious effects of PCOS. However, no systematic network pharmacology analysis of the effectiveness of Danshen has been reported before. Indeed, we previously demonstrated that cryptotanshinone prevents PCOS and was also found to alleviate the reproductive and metabolic disorders in PCOS by regulating the expression of CYP17 and AR *in vivo* (Yu et al., 2014). Randomized clinical trials and systematic *meta*-analysis indicated that tanshinone may also be effective in treating PCOS. Tan-IIA alleviates estradiol-induced PCOS *in vivo* by improving FSHR expression in the ovary (Jin et al., 2019). In addition, a recent *meta*-analysis indicated that Danshen may be effective in treating PCOS. However, the identification and the molecular mechanism of the ingredients of Danshen in PCOS treatment and prevention still need to be explored. To the best of our knowledge, our present study presents for the first time the global overview of the potential Danshen ingredients that could be effective in the protection and treatment of PCOS. In compliance with past studies (Yu et al., 2014, Hong et al., 2017, Jin et al., 2019, Lin et al., 2019, Qin et al., 2022), cryptotanshinone and tanshinones were predicted as important ingredients of Danshen. In addition, novel ingredients that have not been reported to be effective against PCOS were also identified. Thus, the present study uncovered new therapeutic candidate molecules for PCOS treatment.

The effect of Bajitian on PCOS has not been reported so far. Our present study indicated that Bajitian may be efficient against PCOS due to its bioactive ingredients. In addition, we found that the combination of Bajitian and Danshen may be more efficient than single drugs due to the broad range of combined drugs. Thus, preparing and administrating the decoctions based on the combinations of Bajitian and Danshen may be important for treating PCOS.

Among the predicted targets, Tan-IIA was found to be the ingredient with the highest number of targets in PCOS, indicating that this drug may be the most effective bioactive compound in treating PCOS. In addition, the targets of Tan-IIA in PCOS treatment constituted a regulatory network with PTGS2, JUN, FOS, TP53, PTGS2, and CASP3 as the most important genes. Previous studies indicated that Tan-IIA hinders oral squamous cell carcinoma by reducing aerobic glycolysis mediated by the Akt-MYC pathway (Li et al., 2020). Sodium Tan-IIA sulfonate was reported to alleviate Ang II-induced cardiomyocyte hypertrophy via downregulating JUN and FOS in cardiomyocytes (Zhou et al., 2008). Tan-IIA was also reported to hinder osteoclast differentiation by inhibiting the expression of c-Fos and NFATc1(Kwak et al., 2006). Tan-IIA promotes ferroptosis via p53-mediated inhibition of SLC7A11 and upregulation of PTGS2 and CHAC1 expression in gastric cancer (Guan et al., 2020). Tan-IIA induces apoptosis by increasing the expression of TP53 in triple-negative breast cancer (Liu et al., 2023). Combined with Nutlin-3, Tan-IIA exerts a cytotoxicity effect on acute leukemic cells by targeting MDM2-P53 and the AKT/mTOR pathway (Guo et al., 2019). Tan-IIA markedly hindered the expressions of PTGS2 in the peripheral blood of ankylosing spondylitis patients (Fang et al., 2022) and inhibited the expression of CASP3 in cerebral ischemic injury (Zhou et al., 2015). However, the effect of Tan-IIA on these proteins in PCOS has not been reported before. In addition, the involvement of these proteins in PCOS has not been well elucidated. Thus, we further explored the effect of Tan-IIA on the deleterious effect of PCOS and the expression of these hub genes by performing *in vitro* and *in vivo* experiments. We found that Tan-IIA effectively counteracted the deleterious impact of PCOS by inhibiting the FOS/JUN/TP53. To date, only one study has explored the effect of Tan-IIA on PCOS and reported that this molecule attenuates estradiol-induced PCOS by upregulating FSHR expression in mice's ovary tissue (Jin et al., 2019). In the present study, we further showed that Tan-IIA regulates inflammatory and hormonal factors, regulates apoptosis, and TP53, PTGS2, and JUN expression levels in the ovarian tissues via FOS. Tan-IIA was reported to hinder cardiomyocyte apoptosis in doxorubicin-induced cardiotoxicity by promoting DAXX/MEK/ERK1/2 signaling pathway (Xu et al., 2022a). Tan-IIA also promoted apoptosis in acute promyelocytic leukemia cells via the PI3K/Akt/mTOR signaling (Pan et al., 2021). The effect of Tan-IIA on the apoptosis of hepatocytes and various cancer cells has also been reported (Nie et al., 2020, Deng et al., 2021, Zhou et al., 2021, Xu et al., 2022b). However, our study is the first to report the effect of Tan-IIA on apoptosis in PCOS. Though numerous studies have indicated the upregulation of FOS, PTGS2, and JUN in apoptotic cells (Pandey and Wang, 1995, Yuan et al., 2009, Wu et al., 2018, Xiao et al., 2018, Liu et al., 2021, Zhou et al., 2022b), the effects of these proteins on PCOS have not been reported so far. The upregulation of these proteins in PCOS indicated their involvement in PCOS pathogenesis. In addition, the activation of FOS by PMA was correlated with increased apoptosis and upregulation of JUN and TP53 but decreased by Tan-IIA treatment, which suggested that Tan-IIA decreases apoptosis in PCOS by downregulation of JUN and TP53 via FOS inhibition. Our study is also the first to demonstrate that FOS regulates JUN and TP53 in PCOS.

The present study also found that Tan-IIA targets in PCOS were involved in numerous biological processes and pathways. This indicated that Tan-IIA may target these pathways, thereby exerting its therapeutic effect. The role of the vast majority of these pathways in PCOS has not been reported before. G-protein coupled receptors (GPCRs) are important functional molecules in human diseases and are considered key drug targets (Keshelava et al., 2018, Apostolakou et al., 2020). GPCRs function via the β-arrestins and G- proteins to control effectors involved in cellular responses (Keshelava et al., 2018, Apostolakou et al., 2020). Gonadotropin-specific receptors are GPCRs that can convert the FSH and LH signalings into their hormonal actions (Nautiyal et al., 2022). The aryl hydrocarbon receptor (AhR) is a transcription factor involved in various biological processes, such as pathological regulation, immune responses, and development. It was previously demonstrated that

increased expression of AhR in GCs by endoplasmic reticulum stress is involved in the pathogenesis of PCOS (Kunitomi et al., 2021). Macrophage migration inhibitory factor (MIF) is a cytokine regulating the innate immune system and is constitutively expressed in monocytes and macrophages. MIF regulates inflammation and innate immune responses and prevents apoptosis mediated by TP53. MIF hinders p53-induced apoptosis and counteracts NO-induced apoptosis of macrophages. Studies have shown that FSH stimulates the cAMP/PKA signaling and pathways regulated by various kinases. Our study indicated that Tan-IIA targets the above pathways among others in PCOS, suggesting that the mode of action of Tan-IIA was driven via these pathways, among others.

5. Conclusions

The present study demonstrated that the Bajitian and Danshen combination is an effective herbal medicine for treating PCOS. In addition, our results potentiated Tan-IIA as the most active ingredient of the Bajitian-Danshen combination, and its mode of action may be driven through a regulatory network governed by FOS, JUN, TP53, PTGS2, and CASP3. Specifically, Tan-IIA alleviates the deleterious effect of PCOS by targeting the FOS/JUN/TP53 axis. Our current research could be useful as a foundation for exploring the key mechanisms of action of Bajitian-Danshen compounds in the treatment of PCOS. Moreover, there is a need to examine the possible uses of this combination for treating other disorders. Future investigations will need to provide more information about the overall efficacy of this combination and may form a basis for clinical guidance. It is also important to keep in mind the possible side effects and safety issues generally associated with some herbs, namely allergies, drug interactions, bleeding risk, and considerations during pregnancy and lactation.

Author agreement

Honglin Liu, Jiani Xie and Limin Fan performed the network pharmacology analysis and the experiments. Honglin Liu and Jiani Xie wrote the manuscript. Honglin Liu, Jiani Xie, Limin Fan, Jianhua Zhou, Yue Xia, and Xia Peng designed the experiments. Huilan Du and Xiaorong Ni supervised the study. All authors made contributions to this study and gave their approval to the submitted study.

Declaration of competing interest

The authors declare that they have no known competing financial interests or personal relationships that could have appeared to influence the work reported in this paper.

Appendix A. Supplementary data

Supplementary data to this article can be found online at https://doi.org/10.1016/j.arabjc.2024.105641.

References

Amini, L., Mojab, F., Jahanfar, S., et al., 2020. Efficacy of Salvia officinalis extract on the prevention of insulin resistance in euglycemic patients with polycystic ovary syndrome: A double-blinded placebo-controlled clinical trial. Complement Ther Med. 48, 102245 https://doi.org/10.1016/j.ctim.2019.102245.

Apostolakou, A.E., Baltoumas, F.A., Stravopodis, D.J., et al., 2020. Extended Human G-Protein Coupled Receptor Network: Cell-Type-Specific Analysis of G-Protein Coupled Receptor Signaling Pathways. J Proteome Res. 19, 511–524. https://doi.org/10.1021/acs.jproteome.9b00754.

Azziz, R., Carmina, E., Chen, Z., et al., 2016. Polycystic ovary syndrome. Nat Rev Dis Primers. 2, 16057. https://doi.org/10.1038/nrdp.2016.57.

Bednarska, S., Siejka, A., 2017. The pathogenesis and treatment of polycystic ovary syndrome: What's new? Adv Clin Exp Med. 26, 359–367. https://doi.org/10.17219/acem/59380.

Cao, M., Fan, J., Yang, X., et al., 2022. Exploration on Molecular Mechanism of Reversal Effect of Compound Danshen Tablets on Hepatic Fibrosis Based on Network Pharmacology. Appl Bionics Biomech. 2022, 7241719. https://doi.org/10.1155/2022/7241719.

Deng, H., Yu, B., Li, Y., 2021. Tanshinone IIA alleviates acute ethanol-induced myocardial apoptosis mainly through inhibiting the expression of PDCD4 and activating the PI3K/Akt pathway. Phytotherapy Research : PTR. 35, 4309–4323. https://doi.org/10.1002/ptr.7102.

Dong, Y., Zhao, Q., Wang, Y., 2021. Network pharmacology-based investigation of potential targets of astragalus membranaceous-angelica sinensis compound acting on diabetic nephropathy. Scientific Reports. 11, 19496. https://doi.org/10.1038/s41598-021-98925-6.

Fang, Y., Liu, J., Xin, L., et al., 2022. Radix Salvia miltiorrhiza for Ankylosing Spondylitis: Determining Potential Inflammatory Molecular Targets and Mechanism Using Network Pharmacology. BioMed Research International. 2022, 3816258. https://doi.org/10.1155/2022/3816258.

Gao, L., Cao, M., Li, J.Q., et al., 2021. Traditional Chinese Medicine Network Pharmacology in Cardiovascular Precision Medicine. Current Pharmaceutical Design. 27, 2925–2933. https://doi.org/10.2174/1381612826666201112142408.

Gu, X., Ma, Z., Fang, J., et al., 2020. Obesity Enhances Antioxidant Capacity and Reduces Cytokine Levels of the Spleen in Mice to Resist Splenic Injury Challenged by Escherichia coli. J Immunol Res. 2020, 5948256. https://doi.org/10.1155/2020/5948256.

Guan, Z., Chen, J., Li, X., et al., 2020. Tanshinone IIA induces ferroptosis in gastric cancer cells through p53-mediated SLC7A11 down-regulation. Biosci Rep. 40 https://doi.org/10.1042/bsr20201807.

Guo, H., Chen, L., Li, C., et al., 2021. Anti-hyperlipidemic effects of the compound Danshen tablet: roles of antioxidation, anti-inflammation, anticoagulation, and anti-apoptosis. Ann Transl Med. 9, 744. https://doi.org/10.21037/atm-20-7915.

Guo, Y., Li, Y., Wang, F.F., et al., 2019. The combination of Nutlin-3 and Tanshinone IIA promotes synergistic cytotoxicity in acute leukemic cells expressing wild-type p53 by co-regulating MDM2-P53 and the AKT/mTOR pathway. Int J Biochem Cell Biol. 106, 8–20. https://doi.org/10.1016/j.biocel.2018.10.008.

Guo, R., Li, L., Su, J., et al., 2020. Pharmacological Activity and Mechanism of Tanshinone IIA in Related Diseases. Drug Des Devel Ther. 14, 4735–4748. https://doi.org/10.2147/dddt.s266911.

Hart, R., 2008. PCOS and infertility. Panminerva Medica. 50, 305–314.

Hong, M., Li, S., Wang, N., et al., 2017. A Biomedical Investigation of the Hepatoprotective Effect of Radix salviae miltiorrhizae and Network Pharmacology-Based Prediction of the Active Compounds and Molecular Targets. Int J Mol Sci. 18 https://doi.org/10.3390/ijms18030620.

Huang, X., Gao, L., Deng, R., et al., 2023. Huangqi-Danshen decoction reshapes renal glucose metabolism profiles that delays chronic kidney disease progression. Biomed Pharmacother. 164, 114989 https://doi.org/10.1016/j.biopha.2023.114989.

Huang, D., Wen, X., Lu, C., et al., 2022. Investigating the molecular mechanism of Compound Danshen Dropping Pills for the treatment of epilepsy by utilizing network pharmacology and molecular docking technology. Ann Transl Med. 10, 216. https://doi.org/10.21037/atm-22-195.

Hügel, H.M., Jackson, N., 2014. Danshen diversity defeating dementia. Bioorg Med Chem Lett. 24, 708–716. https://doi.org/10.1016/j.bmcl.2013.12.042.

Jiang, W., Chen, X., Guo, M., et al., 2022. Analysis of Fungal Microbiomes in Edible Medicinal Morindae Officinalis Radix and Alpiniae Oxyphyllae Fructus Using DNA Metabarcoding. Foods. 11 https://doi.org/10.3390/foods11121748.

Jiashuo, W.U., Fangqing, Z., Zhuangzhuang, L.I., et al., 2022. Integration Strategy of Network Pharmacology in Traditional Chinese Medicine: a Narrative Review. Journal of Traditional Chinese Medicine = Chung i Tsa Chih Ying Wen Pan. 42, 479–486. https://doi.org/10.19852/j.cnki.jtcm.20220408.003.

Jin, J., Hu, Q.Y., Xu, W.W., et al., 2019. Tanshinone IIA attenuates estradiol-induced polycystic ovarian syndrome in mice by ameliorating FSHR expression in the ovary. Exp Ther Med. 17, 3501–3508. https://doi.org/10.3892/etm.2019.7352.

Jin, P., Xie, Y., 2018. Treatment strategies for women with polycystic ovary syndrome. Gynecological Endocrinology : the Official Journal of the International Society of Gynecological Endocrinology. 34, 272–277. https://doi.org/10.1080/09513590.2017.1395841.

Kang, L., Zhang, Y., Zhou, L., et al., 2021. Structural Characterization and Discrimination of Morinda officinalis and Processing Morinda officinalis Based on Metabolite Profiling Analysis. Front Chem. 9, 803550 https://doi.org/10.3389/fchem.2021.803550.

Keshelava, A., Solis, G.P., Hersch, M., et al., 2018. High capacity in G protein-coupled receptor signaling. Nature Communications. 9, 876. https://doi.org/10.1038/s41467-018-02868-y.

Kumar, R., Malik, S., Tiwari, R., et al., 2021. Pathophysiology of Cardiovascular Diseases and the Role of Vitamins, and Herbal Extracts in the Reduction of Cardiovascular Risks. Cardiovascular & Hematological Agents in Medicinal Chemistry. 19, 175–186. https://doi.org/10.2174/1871525718666201217102638.

Kunitomi, C., M. Harada, J. M. K. Azhary, et al., 2021. Upregulation of Aryl Hydrocarbon Receptor in Granulosa Cells by Endoplasmic Reticulum Stress Contributes to the PCOS Pathophysiology, J Endocr Soc. 2021 May 3;5(Suppl 1):A773. doi: 10.1210/jendso/bvab048.1573.

Kwak, H.B., Yang, D., Ha, H., et al., 2006. Tanshinone IIA inhibits osteoclast differentiation through down-regulation of c-Fos and NFATc1. Exp Mol Med. 38, 256–264. https://doi.org/10.1038/emm.2006.31.

Li, M., Gao, F., Zhao, Q., et al., 2020. Tanshinone IIA inhibits oral squamous cell carcinoma via reducing Akt-c-Myc signaling-mediated aerobic glycolysis. Cell Death & Disease. 11, 381. https://doi.org/10.1038/s41419-020-2579-9.

Li, Z.M., Xu, S.W., Liu, P.Q., 2018. Salvia miltiorrhizaBurge (Danshen): a golden herbal medicine in cardiovascular therapeutics. Acta Pharmacol Sin. 39, 802–824. https://doi.org/10.1038/aps.2017.193.

Li, S., Zhang, B., 2013. Traditional Chinese medicine network pharmacology: theory, methodology and application. Chinese Journal of Natural Medicines. 11, 110–120. https://doi.org/10.1016/s1875-5364(13)60037-0.

Lin, Y.Y., Lee, I.Y., Huang, W.S., et al., 2017. Danshen improves survival of patients with colon cancer and dihydroisotanshinone I inhibit the proliferation of colon cancer cells via apoptosis and skp2 signaling pathway. J Ethnopharmacol. 209, 305–316. https://doi.org/10.1016/j.jep.2017.08.011.

Lin, Y.S., Shen, Y.C., Wu, C.Y., et al., 2019. Danshen Improves Survival of Patients With Breast Cancer and Dihydroisotanshinone I Induces Ferroptosis and Apoptosis of Breast Cancer Cells. Frontiers in Pharmacology. 10, 1226. https://doi.org/10.3389/fphar.2019.01226.

Liu, L., Li, X., Cai, W., et al., 2022b. Coadministration of Compound Danshen dripping pills and bezafibrate has a protective effect against diabetic retinopathy. Frontiers in Pharmacology. 13, 1014991. https://doi.org/10.3389/fphar.2022.1014991.

Liu, M.Y., Luo, Z.H., Chen, Z.E., et al., 2022c. Quality markers for processed products of Morinda officinalis how based on the "oligosaccharides-spectrum-effect". J Pharm Biomed Anal. 208, 114403 https://doi.org/10.1016/j.jpba.2021.114403.

Liu, J., Shi, Y., Peng, D., et al., 2022a. Salvia miltiorrhiza Bge. (Danshen) in the Treating Non-alcoholic Fatty Liver Disease Based on the Regulator of Metabolic Targets. Front Cardiovasc Med. 9, 842980 https://doi.org/10.3389/fcvm.2022.842980.

Liu, Y.Y., Yu, L.H., Zhang, J., et al., 2021b. Network Pharmacology-Based and Molecular Docking-Based Analysis of Suanzaoren Decoction for the Treatment of Parkinson's Disease with Sleep Disorder. BioMed Research International. 2021, 1752570. https://doi.org/10.1155/2021/1752570.

Liu, J., Zhang, C., Liu, S., et al., 2023. Tanshinone IIA promotes apoptosis by downregulating BCL2 and upregulating TP53 in triple-negative breast cancer. Naunyn-Schmiedeberg's Archives of Pharmacology. 396, 365–374. https://doi.org/10.1007/s00210-022-02316-1.

Luo, T.T., Lu, Y., Yan, S.K., et al., 2020. Network Pharmacology in Research of Chinese Medicine Formula: Methodology, Application and Prospective. Chinese Journal of Integrative Medicine. 26, 72–80. https://doi.org/10.1007/s11655-019-3064-0.

Ma, J.C., Wang, Q., Li, B.Y., et al., 2021. Case series analysis of Professor Wang Qi's prescriptions for oligoasthenospermia. Zhonghua Nan Ke Xue. 27, 155–160.

Nautiyal, H., Imam, S.S., Alshehri, S., et al., 2022. Polycystic Ovarian Syndrome: A Complex Disease with a Genetics Approach. Journal. 10 https://doi.org/10.3390/biomedicines10030540.

Nie, Z.Y., Zhao, M.H., Cheng, B.Q., et al., 2020. Tanshinone IIA regulates human AML cell proliferation, cell cycle, and apoptosis through miR-497-5p/AKT3 axis. Cancer Cell Int. 20, 379. https://doi.org/10.1186/s12935-020-01468-5.

Nogales, C., Mamdouh, Z.M., List, M., et al., 2022. Network pharmacology: curing causal mechanisms instead of treating symptoms. Trends in Pharmacological Sciences. 43, 136–150. https://doi.org/10.1016/j.tips.2021.11.004.

Orgah, J.O., He, S., Wang, X., et al., 2020. Pharmacological potential of the combination of Salvia miltiorrhiza (Danshen) and Carthamus tinctorius (Honghua) for diabetes mellitus and its cardiovascular complications. Pharmacol Res. 153, 104654 https://doi.org/10.1016/j.phrs.2020.104654.

Pan, Y., Chen, L., Li, R., et al., 2021. Tanshinone IIa Induces Autophagy and Apoptosis via PI3K/Akt/mTOR Axis in Acute Promyelocytic Leukemia NB4 Cells. Evidence-Based Complementary and Alternative Medicine : Ecam. 2021, 3372403. https://doi.org/10.1155/2021/3372403.

Pandey, S., Wang, E., 1995. Cells en route to apoptosis are characterized by the upregulation of c-fos, c-myc, c-jun, cdc2, and RB phosphorylation, resembling events of early cell-cycle traverse. J Cell Biochem. 58, 135–150. https://doi.org/10.1002/jcb.240580203.

Piao, C.L., Luo, J.L., Jin, D., et al., 2019. Utilizing network pharmacology to explore the underlying mechanism of Radix Salviae in diabetic retinopathy. Chin Med. 14, 58. https://doi.org/10.1186/s13020-019-0280-7.

Pinzi, L., Rastelli, G., 2019. Molecular Docking: Shifting Paradigms in Drug Discovery. Int J Mol Sci. 20 https://doi.org/10.3390/ijms20184331.

Qin, C., Wu, M., Wang, X., et al., 2022. Study on the mechanism of Danshen-Guizhi drug pair in the treatment of ovarian cancer based on network pharmacology and in vitro experiment. PeerJ. 10, e13148.

Shi, Y., Liu, D., Yuan, J., et al., 2020. Compound Danshen Dripping Pills Prevented Leptin Deficiency-Induced Hepatic ER Stress, Stimulated Autophagy, and Improved Insulin Resistance of ob/ob Mice. Evidence-Based Complementary and Alternative Medicine : Ecam. 2020, 5368657. https://doi.org/10.1155/2020/5368657.

Shi, N., Zhou, Y., Ma, H., 2022. A network pharmacology study of mechanism and efficacy of Jiawei Huanglian-Wendan decoction in polycystic ovary syndrome with

insulin resistance. Medicine. 101, e32057–e. https://doi.org/10.1097/MD.0000000000032057.

Tan, F.H.P., Ting, A.C.J., Leow, B.G., et al., 2021. Alleviatory effects of Danshen, Salvianolic acid A and Salvianolic acid B on PC12 neuronal cells and Drosophila melanogaster model of Alzheimer's disease. J Ethnopharmacol. 279, 114389 https://doi.org/10.1016/j.jep.2021.114389.

Wan, H., Yang, Y., Li, Z., et al., 2021. Compatibility of ingredients of Danshen (Radix Salviae Miltiorrhizae) and Honghua (Flos Carthami) and their protective effects on cerebral ischemia-reperfusion injury in rats. Exp Ther Med. 22, 849. https://doi.org/10.3892/etm.2021.10281.

Wang, T., Fu, X., Wang, Z., 2019. Danshen Formulae for Cancer: A Systematic Review and Meta-Analysis of High-Quality Randomized Controlled Trials. Evidence-Based Complementary and Alternative Medicine : Ecam. 2019, 2310639. https://doi.org/10.1155/2019/2310639.

Wang, X., Guo, D., Li, W., et al., 2020b. Danshen (Salvia miltiorrhiza) restricts MD2/TLR4-MyD88 complex formation and signalling in acute myocardial infarction-induced heart failure. J Cell Mol Med. 24, 10677–10692. https://doi.org/10.1111/jcmm.15688.

Wang, L., Ma, R., Liu, C., et al., 2017. Salvia miltiorrhiza: A Potential Red Light to the Development of Cardiovascular Diseases. Current Pharmaceutical Design. 23, 1077–1097. https://doi.org/10.2174/1381612822666161010105242.

Wang, Y., Yang, H., Chen, L., et al., 2021. Network-based modeling of herb combinations in traditional Chinese medicine. Briefings in Bioinformatics. 22, bbab106. https://doi.org/10.1093/bib/bbab106.

Wu, Z.Q., Chen, D.L., Lin, F.H., et al., 2015. Effect of bajijiasu isolated from Morinda officinalis F. C. how on sexual function in male mice and its antioxidant protection of human sperm. J Ethnopharmacol. 164, 283–292. https://doi.org/10.1016/j.jep.2015.02.016.

Wu, P.Y., Chen, W., Huang, H., et al., 2022b. Morinda officinalis polysaccharide regulates rat bone mesenchymal stem cell osteogenic-adipogenic differentiation in osteoporosis by upregulating miR-21 and activating the PI3K/AKT pathway. Kaohsiung J Med Sci. 38, 675–685. https://doi.org/10.1002/kjm2.12544.

Wu, C.Y., Cherng, J.Y., Yang, Y.H., et al., 2017a. Danshen improves survival of patients with advanced lung cancer and targeting the relationship between macrophages and lung cancer cells. Oncotarget. 8, 90925–90947. https://doi.org/10.18632/oncotarget.18767.

Wu, M., Lai, H., Peng, W., et al., 2023. Monotropein: A comprehensive review of biosynthesis, physicochemical properties, pharmacokinetics, and pharmacology. Frontiers in Pharmacology. 14, 1109940. https://doi.org/10.3389/fphar.2023.1109940.

Wu, C.Y., Yang, Y.H., Lin, Y.Y., et al., 2017b. Anti-cancer effect of danshen and dihydroisotanshinone I on prostate cancer: targeting the crosstalk between macrophages and cancer cells via inhibition of the STAT3/CCL2 signaling pathway. Oncotarget. 8, 40246–40263. https://doi.org/10.18632/oncotarget.14958.

Wu, N., Yuan, T., Yin, Z., et al., 2022a. Network Pharmacology and Molecular Docking Study of the Chinese Miao Medicine Sidaxue in the Treatment of Rheumatoid Arthritis. Drug Des Devel Ther. 16, 435–466. https://doi.org/10.2147/dddt.s330947.

Wu, D.M., Zhang, Y.T., Lu, J., et al., 2018. Effects of microRNA-129 and its target gene c-Fos on proliferation and apoptosis of hippocampal neurons in rats with epilepsy via the MAPK signaling pathway. J Cell Physiol. 233, 6632–6643. https://doi.org/10.1002/jcp.26297.

Xiao, P., Liu, X.W., Zhao, N.N., et al., 2018. Correlations of neuronal apoptosis with expressions of c-Fos and c-Jun in rats with post-ischemic reconditioning damage. Eur Rev Med Pharmacol Sci. 22, 2832–2838. https://doi.org/10.26355/eurrev_201805_14984.

Xie, Z., Loi Truong, T., Zhang, P., et al., 2015. Dan-Qi prescription ameliorates insulin resistance through overall corrective regulation of glucose and fat metabolism. J Ethnopharmacol. 172, 70–79. https://doi.org/10.1016/j.jep.2015.05.041.

Xin, G.J., Zhao, Y.W., Li, L.M., et al., 2021. Mechanism of 'Invigorating Qi and Promoting Blood Circulation' Drug Pair Ginseng-Danshen on Treatment of Ischemic Heart Disease Based on Network Pharmacology. Chinese Journal of Integrative Medicine. 27, 440–445. https://doi.org/10.1007/s11655-021-2859-y.

Xu, L., He, D., Wu, Y., et al., 2022a. Tanshinone IIA inhibits cardiomyocyte apoptosis and rescues cardiac function during doxorubicin-induced cardiotoxicity by activating the DAXX/MEK/ERK1/2 pathway. Phytomedicine : International Journal of Phytotherapy and Phytopharmacology. 107, 154471 https://doi.org/10.1016/j.phymed.2022.154471.

Xu, L., Liu, X., Jia, T., et al., 2022b. Tanshinone IIA Ameliorates Nonalcoholic Steatohepatitis in Mice by Modulating Neutrophil Extracellular Traps and Hepatocyte Apoptosis. Evidence-Based Complementary and Alternative Medicine : Ecam. 2022, 5769350. https://doi.org/10.1155/2022/5769350.

Yang, C.Y., Hsieh, C.C., Lin, C.K., et al., 2017. Danshen extract circumvents drug resistance and represses cell growth in human oral cancer cells. BMC Complement Altern Med. 17, 555. https://doi.org/10.1186/s12906-017-2063-y.

Yang, W., Ju, J.H., Jeon, M.J., et al., 2010. Danshen (Salvia miltiorrhiza) extract inhibits proliferation of breast cancer cells via modulation of Akt activity and p27 level. Phytotherapy Research : PTR. 24, 198–204. https://doi.org/10.1002/ptr.2945.

Ye, T., Xiong, D., Chen, L., et al., 2020. Effect of Danshen on TLR2-triggered inflammation in macrophages. Phytomedicine : International Journal of Phytotherapy and Phytopharmacology. 70, 153228 https://doi.org/10.1016/j.phymed.2020.153228.

Ye, T., Li, Y., Xiong, D., et al., 2021. Combination of Danshen and ligustrazine has dual anti-inflammatory effect on macrophages and endothelial cells. J Ethnopharmacol. 266, 113425 https://doi.org/10.1016/j.jep.2020.113425.

Yu, J., Zhai, D., Hao, L., et al., 2014. Cryptotanshinone Reverses Reproductive and Metabolic Disturbances in PCOS Model Rats via Regulating the Expression of CYP17 and AR. Evidence-Based Complementary and Alternative Medicine : Ecam. 2014, 670743 https://doi.org/10.1155/2014/670743.

Yu, H., Zhang, L., Yin, F., et al., 2023. Exploring the molecular targets and mechanism of S. miltiorrhiza-C. aromatica in treating polycystic ovary syndrome based on network pharmacology. Ann Transl Med. 11, 149. https://doi.org/10.21037/atm-23-29.

Yuan, Z., Gong, S., Luo, J., et al., 2009. Opposing roles for ATF2 and c-Fos in c-Jun-mediated neuronal apoptosis. Molecular and Cellular Biology. 29, 2431–2442. https://doi.org/10.1128/mcb.01344-08.

Zhang, J., Liu, S.L., Wang, H., et al., 2021a. The effects of borneol on the pharmacokinetics and brain distribution of tanshinone IIA, salvianolic acid B and ginsenoside Rg(1) in Fufang Danshen preparation in rats. Chinese Journal of Natural Medicines. 19, 153–160. https://doi.org/10.1016/s1875-5364(21)60016-x.

Zhang, Y.-Y., Ma, J.-X., Zhu, Y.-T., et al., 2022c. Investigation of the mechanisms and experimental verification of Cuscuta-Salvia in the treatment of polycystic ovary syndrome (PCOS) via network pharmacology, 40-40 Journal of Ovarian Research. 15. https://doi.org/10.1186/s13048-022-00964-8.

Zhang, Z., Wang, Y., Tan, W., et al., 2019. A Review of Danshen Combined with Clopidogrel in the Treatment of Coronary Heart Disease. Evidence-Based Complementary and Alternative Medicine : Ecam. 2019, 2721413. https://doi.org/10.1155/2019/2721413.

Zhang, C., Xu, T., Lin, L., et al., 2022a. Morinda officinalis Polysaccharides Ameliorates Bone Growth by Attenuating Oxidative Stress and Regulating the Gut Microbiota in Thiram-Induced Tibial Dyschondroplasia Chickens. Metabolites. 12 https://doi.org/10.3390/metabo12100958.

Zhang, D., Zhang, S., Jiang, K., et al., 2020. Bioassay-guided isolation and evaluation of anti-osteoporotic polysaccharides from Morinda officinalis. J Ethnopharmacol. 261, 113113 https://doi.org/10.1016/j.jep.2020.113113.

Zhang, D., Fan, L., Yang, N., et al., 2022b. Discovering the main "reinforce kidney to strengthening Yang" active components of salt Morinda officinalis based on the spectrum-effect relationship combined with chemometric methods. J Pharm Biomed Anal. 207, 114422 https://doi.org/10.1016/j.jpba.2021.114422.

Zhang, J., Zhou, Y., Ma, Z., 2021b. Multi-target mechanism of Tripteryguim wilfordii Hook for treatment of ankylosing spondylitis based on network pharmacology and molecular docking. Ann Med. 53, 1090–1098. https://doi.org/10.1080/07853890.2021.1918345.

Zhou, L., Bondy, S.C., Jian, L., et al., 2015. Tanshinone IIA attenuates the cerebral ischemic injury-induced increase in levels of GFAP and of caspases-3 and -8. Neuroscience. 288, 105–111. https://doi.org/10.1016/j.neuroscience.2014.12.028.

Zhou, D., Liang, Q., He, X., et al., 2008. Changes of c-fos and c-jun mRNA expression in angiotensin II-induced cardiomyocyte hypertrophy and effects of sodium tanshinone IIA sulfonate. J Huazhong Univ Sci Technolog Med Sci. 28, 531–534. https://doi.org/10.1007/s11596-008-0509-7.

Zhou, X., Lv, L., Tan, Y., et al., 2021. Tanshinone IIA sensitizes TRAIL-induced apoptosis in glioblastoma through inducing the expression of death receptors (and suppressing STAT3 activation). Brain Res. 1766, 147515 https://doi.org/10.1016/j.brainres.2021.147515.

Zhou, L., Xue, C., Chen, Z., et al., 2022a. c-Fos is a mechanosensor that regulates inflammatory responses and lung barrier dysfunction during ventilator-induced acute lung injury. BMC Pulm Med. 22, 9. https://doi.org/10.1186/s12890-021-01801-2.

Zhou, W., Zhang, H., Wang, X., et al., 2022b. Network pharmacology to unveil the mechanism of Moluodan in the treatment of chronic atrophic gastritis. Phytomedicine : International Journal of Phytotherapy and Phytopharmacology. 95, 153837 https://doi.org/10.1016/j.phymed.2021.153837.